



PCCP

Dynamics of aggregated states resolved by gated fluorescence in films of room temperature phosphorescent emitters

Journal:	<i>Physical Chemistry Chemical Physics</i>
Manuscript ID	CP-ART-11-2018-007005.R1
Article Type:	Paper
Date Submitted by the Author:	n/a
Complete List of Authors:	dos Santos, Paloma Lays; Durham University, Physics Department Silveira, Orlando; Universidade Federal de Minas Gerais Instituto de Ciencias Exatas, Física Huang, Rogjuan; Durham University, Physics Jardim, Guilherme; Universidade Federal de Minas Gerais, Matos, Matheus; Universidade Federal de Ouro Preto, Fisica da Silva Júnior, Eufrânio; Universidade Federal de Minas Gerais Instituto de Ciencias Exatas, Química Monkman, Andrew; University of Durham, Durham Photonics Institute Dias, Fernando; Univ Durham, Dept Phys Cury, Luiz; Universidade Federal de Minas Gerais, Departamento de Fisica
Note: The following files were submitted by the author for peer review, but cannot be converted to PDF. You must view these files (e.g. movies) online.	
Phenazine-Zeonex Films Gated Fluorescence - DFT - Recorrecao.tex	

SCHOLARONE™
Manuscripts

Article type: Full paper

PCCP

Physical Chemistry Chemical Physics



Website www.rsc.org/pccp

Impact factor* 4.123

Journal expectations To be suitable for publication in *Physical Chemistry Chemical Physics (PCCP)* articles must include significant new insight into physical chemistry.

Article type: Full paper Original scientific work that has not been published previously. Full papers do not have a page limit and should be appropriate in length for scientific content.

Journal scope Visit the [PCCP website](http://www.rsc.org/pccp) for additional details of the journal scope and expectations.

PCCP is an international journal for the publication of cutting-edge original work in physical chemistry, chemical physics and biophysical chemistry. To be suitable for publication in *PCCP*, articles must include significant new insight into physical chemistry; this is the most important criterion that reviewers should judge against when evaluating submissions. Example topics within the journal's broad scope include:

- Spectroscopy
- Dynamics
- Kinetics
- Statistical mechanics
- Thermodynamics
- Electrochemistry
- Catalysis
- Surface science
- Quantum mechanics
- Theoretical research

Interdisciplinary research areas such as polymers and soft matter, materials, nanoscience, surfaces/interfaces, and biophysical chemistry are also welcomed if they demonstrate significant new insight into physical chemistry.

Reviewer responsibilities Visit the [Reviewer responsibilities website](http://www.rsc.org/pccp) for additional details of the reviewing policy and procedure for Royal Society of Chemistry journals.

When preparing your report, please:

- Focus on the originality, importance, impact and reliability of the science. English language and grammatical errors do not need to be discussed in detail, except where it impedes scientific understanding.
- Use the [journal scope and expectations](http://www.rsc.org/pccp) to assess the manuscript's suitability for publication in *PCCP*.
- State clearly whether you think the article should be accepted or rejected and include details of how the science presented in the article corresponds to publication criteria.
- Inform the Editor if there is a conflict of interest, a significant part of the work you cannot review with confidence or if parts of the work have previously been published.

Thank you for evaluating this manuscript, your advice as a reviewer for *PCCP* is greatly appreciated.

Dr Katie Lim Executive Editor
Royal Society of Chemistry, UK

Professor Seong Keun Kim Editorial Board Chair
Seoul National University, South Korea

Belo Horizonte, January 16 2019.

To Dr. A. Ajayaghosh
Associate Editor
Physical Chemistry Chemical Physics
E-mail: ajayaghosh@niist.res.in

Dear Dr. Ajayaghosh,

This letter is concerned to our manuscript ID: CP-ART-07-2018-004449, entitled “**Dynamics of aggregated states resolved by gated fluorescence in films of room temperature phosphorescent emitters**”, which has been revised in order to fill the requirements of the reviewers.

Dear Reviewers,

We would like to thank you for your constructive contributions towards this manuscript. Below we have addressed all of your comments and have also made any necessary amendments to the revised manuscript (changes made in blue in the text) and supplementary information.

Referee: 1

Comments to the Author

This revision has partially responded my concerns. Actually, the obtaining of photophysical properties (emission spectrum, fluorescence lifetime and quantum yield) for real monomer emission is a very important starting point for the study. The spectrum carefully check the both the absorption and fluorescence spectra for the solutions concentrations ranging from 0.0001-0.001 mg/mL (preferably molar concentrations), presenting both the fluorescence and the absorption spectra scaling molar extinction coefficient rather than absorbance vs. wavelength. Since the emission is much more sensitive than the absorption, and more logically performed.

We agree with the referee that the data for a real monomer is important in this study. This is the reason we have included the emission spectra of solutions in different concentrations (Figure S1) in the last version of the manuscript. The shoulder observed in the emission spectra (Figure S1) refers to a vibronic peak and it is not related to aggregation.

In an early publication, the vibrational mode corresponding to the shoulder was identified around 1540 cm^{-1} by Raman spectroscopy and infrared absorption.¹ This vibrational mode and neighbour modes that could contribute to that vibronic band are in the $1300\text{--}1600\text{ cm}^{-1}$

range, where the CC stretching vibrations of the phenazine core rings of the probe molecule are expected.^{2,3}

1. B. B. A. Costa, P. D.C. Souza, R. Gontijo, G. A. M. Jardim, R. L. Moreira, E. N. da Silva Júnior, L. A. Cury, Chem. Phys. Lett. 695 (2018) 176. See Figures S2b and S3 of the respective Supplementary Information.
2. A. Wheaton, L.J. Stoel, N.B. Stevens, C.W. Frank, Appl. Spectroscopy 24 (1970) 339.
3. R.J. Kessler, M.R. Fisher, G.N.R. Tripathi, Chem. Phys. Lett. 112 (1984) 575.

We have added in the revised supplementary information the absorption and emission spectra with concentrations ranging from 0.0001 - 0.1 mg/mL (see Figures S1a and S1b). Note the shoulder around 470 nm appears in all of the PL spectra (Figure S1b). The peak positions of absorption spectra are the same (Figure S1a), being the more important feature to be analysed rather than molar extinction coefficient. At 0.0001 mg/mL, the absorbance signal is very faint and the curve was smoothed for better comparison.

We believe the fluorescence lifetime and quantum yield for solutions are not relevant for this study as this study focus on the aggregation formation when the Probe molecules are dispersed in solid state.

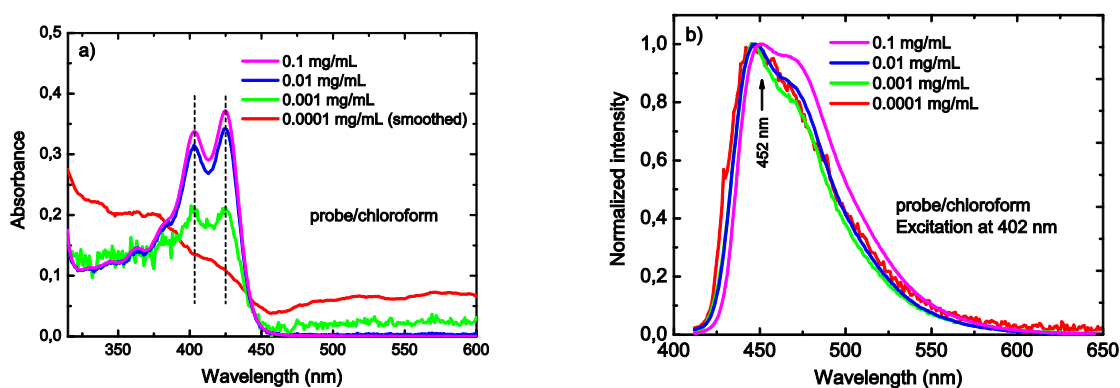


Figure S1 - (a) Absorption and (b) Emission spectra at relatively low concentration of probe solutions in chloroform.

The singlet and triplet energies should also be reported, which could be derived from the low-temperature spectra at 77 K.

We have added the singlet (E_{FL}) and triplet (E_{PH}) energy values in the revised manuscript. These energies were obtained from the onset of the emission spectra of film B₂ at 79 K. The spectrum below shows the steady-state emission with the FL and PH contributions as well as the onset lines indicating the respective energy values E_{FL} and E_{PH} .

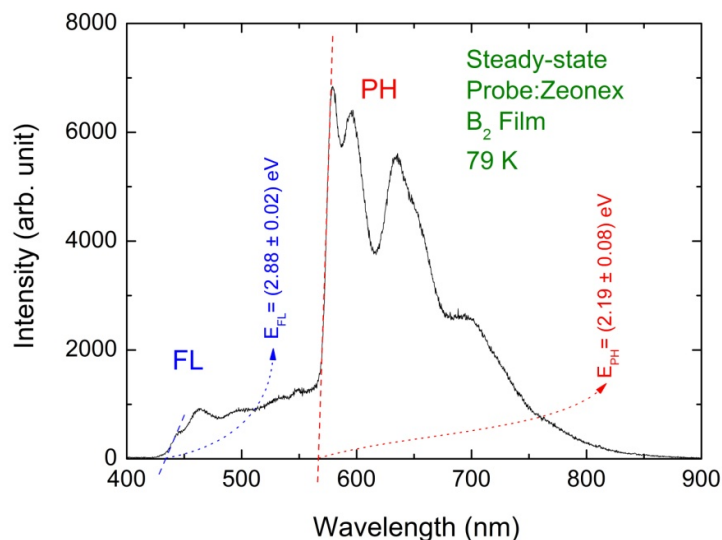


Figure S2 - Steady-state emission spectrum of film B₂ at 79 K. The FL and PH energies, indicated by arrows, were estimated from the respective onset lines.

There is no solid evidences for formation of dimer (Table 1) rather than higher aggregates. From Table 1, aggregation should result in enhanced lifetimes, but they observed intensity enhancement.

All the films show monomer and dimer contribution. Their respective molecular structures are considered similar for both films B₂ and B₄. The change in the intensity of each contribution for different films occurs according to the level of aggregation formation. The aggregate states show indeed enhanced lifetime, note the monomer has lifetime < 0.31 ns and the dimer > 2.2 ns (Table 1). This is certainly a strong support for the dimer formation, beyond the effect of aggregation observed in the absorption measurements. Moreover, the dimer formation is confirmed by the DFT calculations, which represents a reinforcement for our experimental results.

The conclusion part should clearly tell the reader how they controlled experimental conditions to improve photophysical properties of the probe.

We have rewritten the final paragraph of the conclusion as:

"In summary, the strong dependence of the emission dynamics of singlet and triplet states of phenazine derivatives on molecular aggregation was demonstrated in this work. The different preparation conditions of the films leads to the observation of relatively large PLQY and relatively strong room temperature phosphorescence in the more viscous films containing Zeonex. In other words, films with the minimum contribution of aggregates must present enhanced photophysical properties with much lower TTA and non-radiative losses. Thus, the higher dilution of the probe molecule in Zeonex, as used in film B₂, was essential to achieve

these conditions. The results presented here have a direct importance concerning potential applications, in particular, purely organic phosphorescent light emitting diodes."

Ref 38 and 39 are duplicate

In the revised version of the manuscript this was corrected.

Referee: 3

Comments to the Author

In their manuscript entitled "Dynamics of aggregated states resolved by gated fluorescence in films of room temperature phosphorescent emitters", Cury and co-workers studied dynamics of phenazine molecular derivative in the aggregate state using steady state and time resolved fluorescence techniques. The aggregates in the films were prepared by changing the concentration of the compound by blending with Zeonex polymer. The effect of aggregation on the dynamics of the singlet emission as well as the triplet emission were discussed. Formation of aggregate as dimers is identified by time dependent density functional theory calculations. Response by the authors to both the reviewers is convincing as they have made significant improvements in the revised manuscript. Manuscript can be published in PCCP after major revision. The following concerns have to be addressed during the revision.

Concerns:

1. The authors have mentioned "UVVis absorption" in several places. "UVVis absorption" has to be modified as "UV-Vis absorption".

We have made the corrections.

2. The authors have mentioned, "(TDDFT)" in several places. , "(TDDFT)" has to be modified as "(TD-DFT)".

We have made the corrections.

3. Figure 2a, 3a and 4, "fluorescence" has to be corrected as "time resolved fluorescence".

We have made the corrections.

4. Figure 2a, 3a and 4, authors have to mention whether time resolved fluorescence spectra is deconvoluted or not and also the instrument response function (IRF).

Only TCSPC decays can be deconvoluted. In our case, because the IRF of our TCSPC system is relatively low (24 ps) we did not consider the deconvolution process. The decay analysis were made by using a computational program. In the captions of Figures 2 and 3 we have added the text "Deconvolution process of the decays were not considered due to the relatively low instrument response function (IRF) of the TCSPC system (24 ps). The pulse curves, representing the IRF, are shown just for the completeness sake."

5. Figure 2 and 3, the fluorescence lifetime measurement (TCSPC) and time resolved fluorescence spectra (LKS) of monomer and dimer do not correlate well. Why does dimer species show fluorescence spectra at 50 ns delay time when its average lifetime is 2.3 ns (figure 2a).

The TCSPC measurements are made using a pulsed laser with a relatively high repetition rate of 80 MHz (~12.5 ns) for excitation. In this case we are only able to observe recombination processes corresponding to times lower than 12.5 ns. This is a limitation imposed by the TCSPC equipment used for relatively fast decays. This does not mean that recombinations at higher times can not occur. For recombinations occurring at larger times we have used Delayed Fluorescence (DF) technique, where the excitation is made by a different pulsed laser with a repetition rate of 10 Hz (~0.1 s). In this case recombinations ranging from tens of ns up to ms can be measured. The TCSPC decays (Figs. 2b, 2c and 3b) were acquired just to know faster recombination times involved for monomers and dimers. In Figs. 2a and 3a, the spectra were obtained by DF and were made to have an idea of how much longer the monomer and dimer states survive or when they appear or disappear.

6. Figure 6 d and e, theoretical absorption spectra (monomer and dimer) colour has to be changed for the better understanding.

We have made the correction.

7. Time resolved fluorescence spectra of probe solution has to be included in SI.

We believe the time resolved fluorescence spectra of solutions are not relevant for this study as this study focus on the aggregation formation when the Probe molecules are dispersed in solid state. The emission spectra of monomer specie are already identified in the steady state measurements (Figure S1b). A more complete study of probe solution is published in B. B. A. Costa, G. A. M. Jardim, P. L. Santos, H. D. R. Calado, A. P. Monkman, F. B. Dias, E. N. da Silva Júnior, L. A. Cury, Phys. Chem. Chem. Phys. 19, 3473 (2017).

8. Page 7, left side, "with peak emission around 430 nm." Emission maximum does not seem to be around 430 nm in SI Figure 1.

The reviewer is correct. The Figure S1 was replaced by Figure S1b, which is shown above in this response letter. The peak emission for the case at 0.1 mg/mL is around 452 nm and decreases around to 446 nm at 0.0001 mg/mL.

Dynamics of aggregated states resolved by gated fluorescence in films of room temperature phosphorescent emitters

Paloma L. dos Santos^{1‡}, Orlando J. Silveira², Rongjuan Huang¹, Guilherme A. M. Jardim³, Matheus J. S. Matos⁴, Eufrânio N. da Silva Júnior³, Andrew P. Monkman¹, Fernando B. Dias¹, Luiz A. Cury^{2†}

¹*Department of Physics, University of Durham, South Road DH1 3LE, Durham, United Kingdom*

²*Instituto de Ciências Exatas, Departamento de Física, Universidade Federal de Minas Gerais, 31270-901, Belo Horizonte, Minas Gerais, Brazil*

³*Instituto de Ciências Exatas, Departamento de Química, Universidade Federal de Minas Gerais, 31270-901, Belo Horizonte, Minas Gerais, Brazil*

⁴*Instituto de Ciências Exatas e Biológicas, Departamento de Física, Universidade Federal de Ouro Preto, 35400-000, Ouro Preto, Minas Gerais, Brazil*

(Dated: January 15, 2019)

Phenazine derivative molecules were studied using steady state and time resolved fluorescence techniques and demonstrated to lead to strong formation of aggregated species, identified as dimers by time dependent density functional theory calculations. Blended films in a matrix of Zeonex[®], produced at different concentrations, showed different contributions of dimer and monomer emissions in the prompt time frame, e.g. less than 50 ns. In contrast, the phosphorescence (e.g. emission from the triplet state) shows no significant effect on dimer formation, although strong dependence of the phosphorescence intensity on concentration is observed, leading to phosphorescence being quenched at higher concentration.

I. INTRODUCTION

The study of molecular photophysics in solid films has gained strong interest over the past 20 years due to their relevance for the performance of many devices in the molecular optoelectronics field, such as organic light emitting diodes (OLEDs). The luminescence properties of thin films of organic molecules, however, require extensive characterization, since film morphology, molecular structure, packing conditions and the presence of aggregated species, among other effects, have strong influence on the optical and charge transport properties of organic compounds.^{1–7} In the particular area of OLEDs, the improvement of luminescence yields and triplet harvesting properties is key to boost devices performance. For example, improving the OLEDs efficiency is often attempted by trying to maintain strong luminescence yields, while trying to facilitate triplet states to contribute to the production of electroluminescence. Heavy-metal complexes are a class of materials with potential to solve this dilemma, by exploring the strong spin-orbit coupling created by the presence of the heavy-atom leading to emission directly from the triplet state. However, while successful these materials are also prone significant degradation in the blue region, and may create environmental problems when used in high-production output technologies, such as displays and lighting. Metal-free compounds are thus very attractive for application in OLEDs, subsequently they are able to harvest triplet

states and show sufficient strong luminescence yield in solid state.

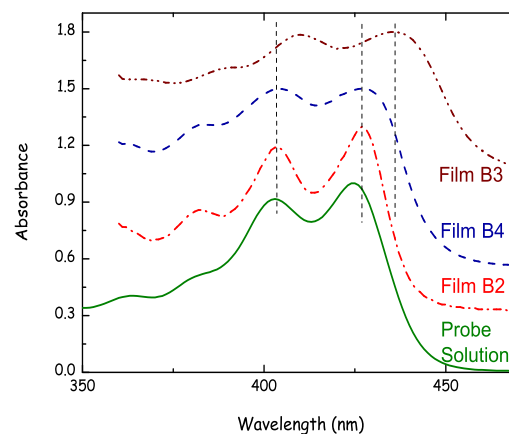


FIG. 1: (Color Online) The normalized UV-Vis absorption spectra for the neat film B_3 (dashed-dotted-dotted line), for the probe:Zeonex[®] blended film B_4 (dashed line), for the probe:Zeonex[®] blended film B_2 (dashed-dotted line), and for the solution of the probe molecule at 0.1 mg/mL in $CHCl_3$ (solid line), at room temperature. The spectra were displaced from each other for clarity sake.

Thermally activated delayed fluorescence reemerged recently as a successful way to promote triplet harvesting (TADF) in metal-free organic compounds. In OLEDs using TADFs the 75% triplet states that are created upon charge recombination are up-converted to the singlet manifold via thermally-activated reverse intersystem crossing. This mechanism gives origin to delayed fluores-

[‡]1st corresponding author. Paloma Lays dos Santos (p.l.dos-santos@durham.ac.uk)

[†]2nd corresponding author. Luiz Alberto Cury (cury@fisica.ufmg.br)

cence, allowing the device internal quantum efficiency to increase up to 100%, in contrast with the maximum 25% that would be otherwise obtained.

Related with the TADF mechanism, the possibility of obtaining direct room temperature phosphorescence (RTP) from metal-free organic compounds has also promoted strong interest in many applications, such as imaging, oxygen sensing, anti-counterfeit labelling, and even OLEDs. Strong RTP is difficult to achieve in metal-free compounds due to the spin forbidden character of phosphorescence, which makes the triplet excited state likely to suffer non-radiative deactivation caused by vibrations and energy transfer to oxygen, among other quenching processes. RTP emitters, therefore, should have high triplet formation yield, which is usually accomplished by the inclusion of heteroatoms in the molecular structure. Nitrogen and Sulphur in particular are effective in creating strong spin-orbit interactions involving $n\pi^*$ transitions, in conformity with El-Sayed's rule. Besides strong triplet formation yields, the observation of strong RTP requires also weak vibrational luminescence quenching. This is mostly accomplished using the influence of intermolecular interactions in crystals and aggregates. However, there are also examples where RTP has been observed in single molecules in isolation, when dispersed in suitable host, such as PMMA or Zeonex[®].^{8,9} In contrast, the observation of RTP from metal-free compounds in liquid phase is extremely rare and intriguing. We are aware of just a few cases, including the case of a phenazine derivative reported recently in our groups.^{5,10} This clearly shows that a systematic understanding of structure-property relationships to create RTP emitters is still lacking.

In this work we report the steady state and time resolved optical spectroscopy studies on a phenazine-based 1,2,3-triazole probe molecule, which shows strong room temperature phosphorescence.¹⁰⁻¹⁵ Samples showing different levels of intermolecular interactions were studied in solution and solid state (neat and blended films using Zeonex[®] host), seeking to unravel the role of aggregate species on the origin of RTP in this phenazine derivative. The results enabled us to observe the presence of different species emitting from their singlet state, with different time resolved fluorescence (TRFL) forms appearing at different delay times, and corresponding to distinct singlet state fluorescence decays. Time dependent density functional theory (TD-DFT) was also employed and the absorption spectra of the monomer and aggregate (dimer) species of the probe molecule were calculated. The comparison of the theoretical and experimental absorption bands strongly indicates that the formation of molecular dimers are the origin of the distinct fluorescence spectra.

Differently from TRFL very similar phosphorescence (PH) spectra and decays were observed for the blended films at different concentrations, therefore, revealing that in contrast with the singlet emission the triplet state is much less affected by the formation of dimers. The

larger difference in this sense was perceived by the decrease of the phosphorescence quantum yield (QY) for the higher concentration sample, revealing a quenching effect on phosphorescence due to concentration.

II. SAMPLES AND EXPERIMENTAL DETAILS

The available natural lapachol compound, extracted from the heartwood of *Tabebuia sp.* (Tecoma) has been used to synthesized the phenazine-based 1,2,3-triazole luminescent and phosphorescent probe molecule investigated in this work. The synthetic route of this derivative phenazine molecule is described in details in the literature.¹⁶

Dropcast films, B_2 and B_4 , were produced respectively from two Probe:Zeonex[®] blend chloroform ($CHCl_3$) solutions, S_2 and S_4 , deposited on glass substrates at room temperature. The blend solution S_2 was prepared adding 366 mg of Zeonex[®] into 5 mL of a probe solution in $CHCl_3$ with 0.1 mg/mL concentration. The blend solution S_4 was prepared adding 1 mL of a probe solution with 3.0 mg/mL concentration in $CHCl_3$ to 4 mL of a Zeonex[®] $CHCl_3$ solution with 71 mg/mL concentration. Considering just the amount of the probe molecule in $CHCl_3$ volume, the final concentrations for the solutions S_2 and S_4 are respectively 0.1 mg/mL and 0.6 mg/mL. Both solutions were left stirring for at 24 h. The Zeonex[®] cyclo-olefin polymers (ZEON Corporation) is an optically inert matrix used to disperse the probe molecules. After drying the solvent, the Zeonex[®] matrix provides a strong rigid medium for the probe molecules in the films. TRFL and PH spectra for the B_2 and B_4 films, obtained in vacuum (10^{-4} Torr) and at room temperature, were recorded using nanosecond and millisecond gated fluorescence acquisition. The excitation source was a high-energy pulsed Nd:YAG laser emitting at 355 nm (EKSPILA). Emissions were focused onto a spectrograph and detected on a sensitive gated iCCD camera (Stanford Computer Optics) having sub-nanosecond resolution. TRFL and PH time resolved measurements were performed by increasing integration and delay times. TRFL decays for the films B_2 and B_4 were also collected using the picosecond time correlated single photon counting (TCSPC) technique (instrument response function 24 ps). In this case, the films were excited by a second harmonic pulse ($\lambda = 394$ nm, 76 MHz of repetition rate) from a mode-locked Ti:sapphire laser from Coherent Inc., with vertical polarization. The emission was detected through a double-subtractive monochromator (SpectraPro-2300i), and a MCP detector (Hamamatsu model R3809U-50) was used to collect decays at different wavelengths. UV-Vis absorption measurements of the blended films B_2 , B_4 , the neat film B_3 , and for a reference probe solution in $CHCl_3$, at relatively low concentration (0.1 mg/mL), were performed at room temperature in a spectrophotometer Shimadzu, model 3600. The drop-casting neat film B_3 on glass substrate, made from

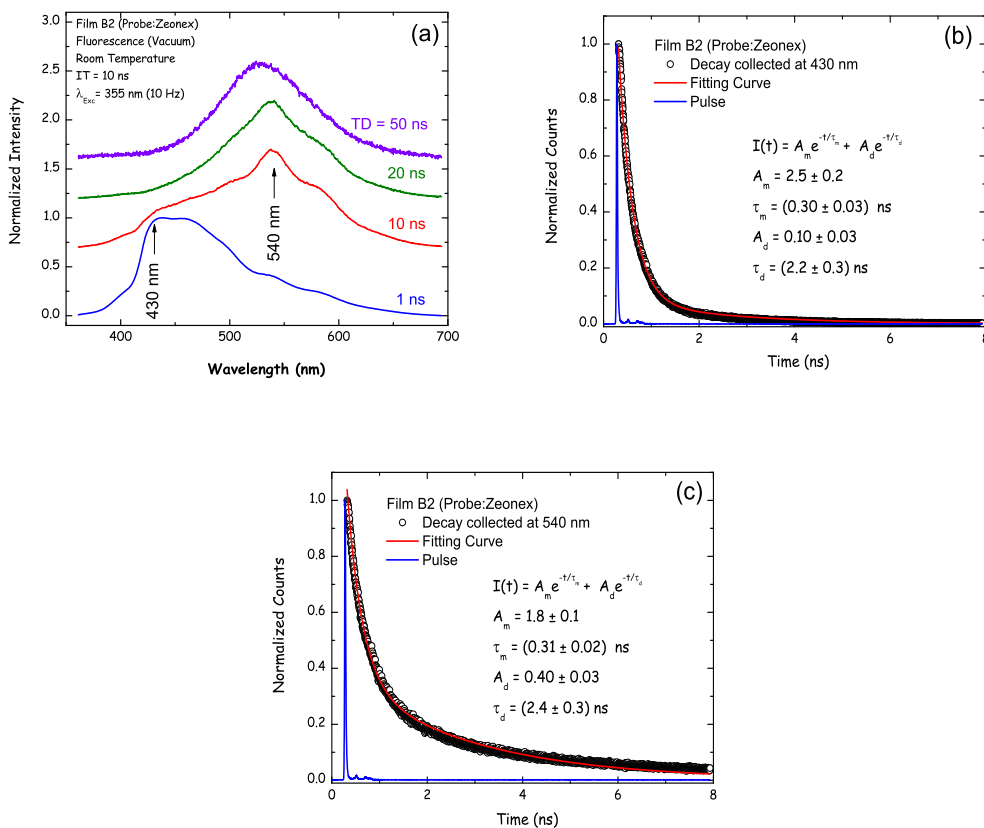


FIG. 2: (Color Online) (a) Time resolved fluorescence (TRFL) spectra obtained for the film B_2 at time delays (TDs) of 1 ns, 10 ns, 20 ns and 50 ns. The TRFL measurements were performed at room temperature, under vacuum, with the excitation made by a 355 nm pulsed laser line (repetition rate of 10 Hz). The spectra were normalized and displaced from each other for clarity sake. The integration time (IT) of 10 ns was used in all measurements; (b) Time correlated single photon counting (TCSPC) decay obtained for the film B_2 with emission collected at 430 nm; (c) TCSPC decay obtained for the film B_2 with emission collected at 540 nm. The TCSPC decays were obtained with the excitation made by a second harmonic pulsed laser ($\lambda = 394$ nm, 76 MHz of repetition rate) from a mode-locked Ti:sapphire laser, Coherent Inc.. The corresponding lifetime components (τ_m and τ_d), obtained by fitting the decay data (solid lines) in (b) and (c), are shown in the respective insets. Deconvolution process of the decays in parts (b) and (c) were not considered due to the relatively low instrument response function (IRF) of the TCSPC system (24 ps). The pulse curves in (b) and (c), representing the IRF, are shown just for the completeness sake.

a probe solution at 3.0 mg/mL in $CHCl_3$, was measured for the sake of aggregation effect comparison.

III. RESULTS AND DISCUSSIONS

Figure 1 shows the normalized absorption spectra of phenazine-based 1,2,3-triazole molecules in solution and solid state. The comparison among these spectra indicates the presence of aggregates in the films, as suggested by the slight red shift observed from solution to blended Zeonex[®] films (weak aggregation effect) and further in neat film (strong aggregation effect). The red shift is probably due to the presence of relatively longer conjugated regions in the molecular aggregates, when com-

pared with the single molecules.^{5,17} Importantly, as the effect of aggregation is observed in the absorption it is therefore associated with the grounded state, rather than formation of excimers, which occurs just in the excited state, and shows no signature in absorption spectra. It is also important to notice in Fig. 1 that for the stronger aggregation effect observed for the neat film B_3 , beyond the effective redshift, a clear broadening of the absorption bands occurs, which is also observed for the blended film B_4 (high concentration) but relatively less for the film B_2 (low concentration), as expected due to its weaker character of aggregation. Figure S1a in the supplementary materials shows the absorption spectra of phenazine-based 1,2,3-triazole molecules in solution at relatively lower concentrations just for comparison.

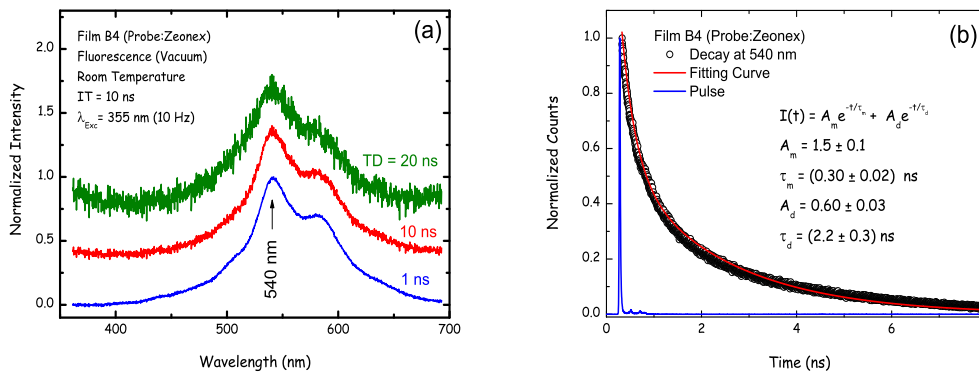


FIG. 3: (Color Online) (a) TRFL spectra obtained for the film B_4 at time delays (TD) of 1 ns, 10 ns, and 20 ns. The TRFL measurements were performed at room temperature, under vacuum, with the excitation made by a 355 nm pulsed laser line (repetition rate of 10 Hz). The spectra were normalized and displaced from each other for clarity sake. The integration time (IT) of 10 ns was used in all measurements; (b) Time correlated single photon counting (TCSPC) decay obtained for the film B_4 at 540 nm. The TCSPC decay was obtained with the excitation made by a second harmonic pulsed laser ($\lambda = 394$ nm, 76 MHz of repetition rate) from a mode-locked Ti:sapphire laser, Coherent Inc.. The corresponding lifetime components (τ_m and τ_d), obtained by fitting the decay data (solid line), are shown in the inset. Deconvolution process of the decay in part (b) was not considered due to the relatively low instrument response function (IRF) of the TCSPC system (24 ps). The pulse curve in (b), representing the IRF, is shown just for the completeness sake.

Film	Monomer			Dimer		
	A_m	τ_m (ns)	W_m	A_d	τ_d (ns)	W_d
B_2 at 430 nm	(2.5 ± 0.2)	(0.30 ± 0.03)	0.77	(0.10 ± 0.03)	(2.2 ± 0.3)	0.23
B_2 at 540 nm	(1.8 ± 0.1)	(0.31 ± 0.02)	0.37	(0.40 ± 0.03)	(2.4 ± 0.3)	0.63
B_4 at 540 nm	(1.5 ± 0.1)	(0.30 ± 0.02)	0.25	(0.60 ± 0.03)	(2.2 ± 0.3)	0.75

TABLE I: Pre-exponential factors A_m and A_d , the corresponding lifetimes τ_m and τ_d , and the corresponding weights W_m and W_d for monomer and dimer contributions obtained from the decay curves (Figs. 2 and 3) at room temperature for the films B_2 and B_4 , respectively. The weights are calculated by $W_m = A_m \tau_m / [A_m \tau_m + A_d \tau_d]$ and $W_d = A_d \tau_d / [A_m \tau_m + A_d \tau_d]$.

To further investigate the formation of aggregates in phenazine-based 1,2,3-triazole films, time resolved emission spectra in the nanosecond time frame were obtained. The TRFL spectra at different time delays (TDs) for film B_2 (0.1 mg/ml phenazine-based 1,2,3-triazole in Zeonex[®]) are shown in Fig. 2a.

The TRFL spectrum at $TD = 1$ ns (Fig. 2a) shows an emission spectrum with a maximum intensity at 430 nm. The steady-state photoluminescence spectra for probe solutions in $CHCl_3$ at relatively lower concentrations, shown in Fig. S1b in the supplementary materials, are representatives of a more monomeric character of the probe emission. The difference for the peak emission, around 450 nm for lower concentration solutions and that at 430 nm for film B_2 is a consequence of different conformational molecular states. Thus, the emission in film B_2 is therefore, mostly assigned to the monomeric form of phenazine-based 1,2,3-triazole. However, a shoulder around 540 nm is also observed, showing that the emission at 1 ns is not purely from the monomer species.

With increasing time delay, the TRFL spectra consecutively changes shape, showing clear displacement from blue to the green region with time (peak around 540 nm), but still presenting a weak shoulder around 430 nm. Finally, at later times ($TD = 50$ ns) the predominant emission shows a Gaussian-type emission peaking around 540 nm, and no shoulder at 430 nm is observed. The film B_2 is formed by a relatively low concentration of phenazine-based 1,2,3-triazole molecules, randomly dispersed in the Zeonex[®] matrix. In these conditions, both monomer and aggregated (dimer) forms can be observed. Their corresponding energies are between the singlet [$E_{PL} = (2.88 \pm 0.02)$ eV (≈ 430 nm)] and triplet [$E_{PH} = (2.19 \pm 0.08)$ eV (≈ 566 nm)] energies, obtained from the onset lines of steady-state emission spectrum of film B_2 at 79 K, as shown in Fig. S2 in the supplementary materials.

The TCSPC decay collected at 430 nm and 540 nm for the film B_2 , are shown, respectively, in Figs. 2b and 2c. The decay at 430 nm shows two clear pre-exponential

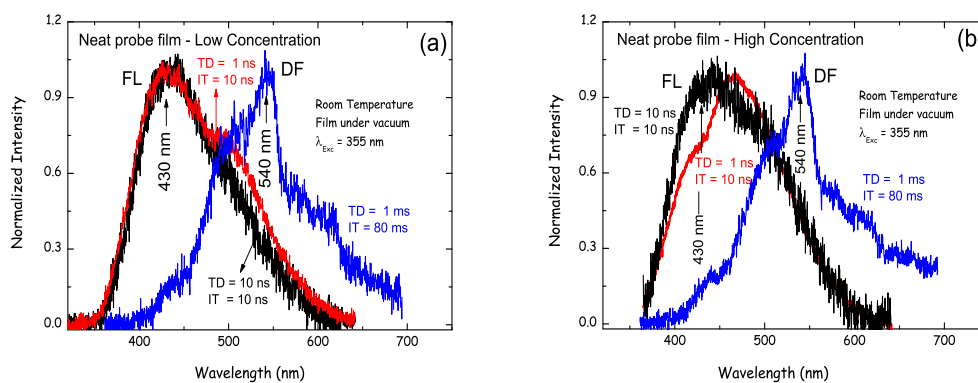


FIG. 4: (Color Online) (a) Normalized time resolved fluorescence (TRFL) spectra of the probe neat film made from the low concentration (0.1 mg/mL) probe solution at $TD = 1 \text{ ns}$ and 10 ns with $IT = 10 \text{ ns}$, and the delayed fluorescence (DF) spectrum at $TD = 1 \text{ ms}$ and $IT = 80 \text{ ms}$; (b) Normalized TRFL spectra of the probe neat film made from the high concentration (3.4 mg/mL) probe solution at $TD = 1 \text{ ns}$ and 10 ns with $IT = 10 \text{ ns}$, and the DF spectrum at $TD = 1 \text{ ms}$ and $IT = 80 \text{ ms}$. The measurements of TRFL and DF spectra in (a) and in (b) were performed at room temperature, under vacuum, with the excitation made by a 355 nm pulsed laser line (repetition rate of 10 Hz).

components (A_m and A_d) and is, therefore, associated with two distinct lifetimes, $\tau_m = (0.30 \pm 0.03) \text{ ns}$ and $\tau_d = (2.2 \pm 0.3) \text{ ns}$, with contribution weights to the overall emission of $W_m = 0.77$ and $W_d = 0.23$, respectively. The faster decay component (τ_m) is associated with the monomer emission, and contributes with most of emission collected at 430 nm , as expected. The longer lifetime (τ_d) is thus associated with the dimer species and dominates the decay collected at 540 nm . This emission also shows bi-exponential decay, $\tau_m = (0.31 \pm 0.02) \text{ ns}$ ($W_m = 0.37$) and $\tau_d = (2.4 \pm 0.3) \text{ ns}$ ($W_d = 0.63$), but with relatively stronger weight of the long-lived decay component.

For the film B_4 , with the higher concentration, and thus, higher degree of intermolecular interaction between phenazine-based 1,2,3-triazole molecules, the TRFL spectrum obtained at initial delay time, $TD = 1 \text{ ns}$, (Fig. 3a), shows the maximum emission intensity position already displaced to the green region, peaking at 540 nm . With increasing time delay, the shape of the TRFL spectra remains practically unchanged. The TRFL corresponding to the dimer form is thus predominant since early times in the B_4 film. This is also strongly supported by the increased contribution of the longer decay component (τ_d), which now represents a weight $W_d = 0.75$ of the overall emission (Fig. 3b). Table 1 shows the pre-exponential factors, the lifetimes, and weights, associated to each exponential (monomer and dimer) for both blended films B_2 and B_4 , highlighting the contributions of monomer and dimer in each sample.

Figures 4a and 4b show the TRFL emission spectra for neat films made from low (0.1 mg/mL) and high (3.4 mg/mL) concentration probe solutions. In both cases the aggregated form would be expected to be pre-

dominant due to the absence of Zeonex[®] host. Surprisingly, the emissions collected at early time delays ($TD = 1 \text{ ns}$ and 10 ns) in both, show predominance of monomer emission, with intensity peaking around 430 nm , and only at late time ($TD = 1 \text{ ms}$) the emissions from aggregates around 540 nm are observed. It is well known that Zeonex[®] is very effective on suppressing molecular vibrations, which makes it a very effective host for observation of RTP.⁵ However, in the absence of Zeonex[®] molecular vibrations may contribute for aggregate dissociation making the monomer form dominant in neat films. The overall emission observed in these neat films are very weak compared to the blended probe:Zeonex[®] films (Figs. 2a and 3a). This is a result of the strong emission quenching of the excited states by the packing conditions in neat films, where non-radiative vibrational mode emissions take place effectively. Consequently, the corresponding PLQYs at steady-state conditions of the neat films are observed to be relatively lower than those of blended probe:Zeonex[®] films, as reported before.⁵

The room temperature phosphorescence spectra of phenazine-based 1,2,3-triazole dispersed in Zeonex[®] at two different concentrations (blended films B_2 and B_4) are shown in Fig. 5a. Strong RTP emission is observed as Zeonex[®] is very effective on suppressing vibrations, allowing PH to compete with non-radiative decay processes that may quench the triplet excited state population. It is also worth mentioning that the PH dominates the steady-state emission, even at room temperature, in both B_2 and B_4 films. Moreover, Zeonex[®] also separates phenazine-based 1,2,3-triazole molecules, minimizing the occurrence of triplet-triplet annihilation (TTA), which would also compete against the PH emission.

The PH decays for both B_2 and B_4 films show bi-exponential profiles (see Figs. 5b and 5c), with decay

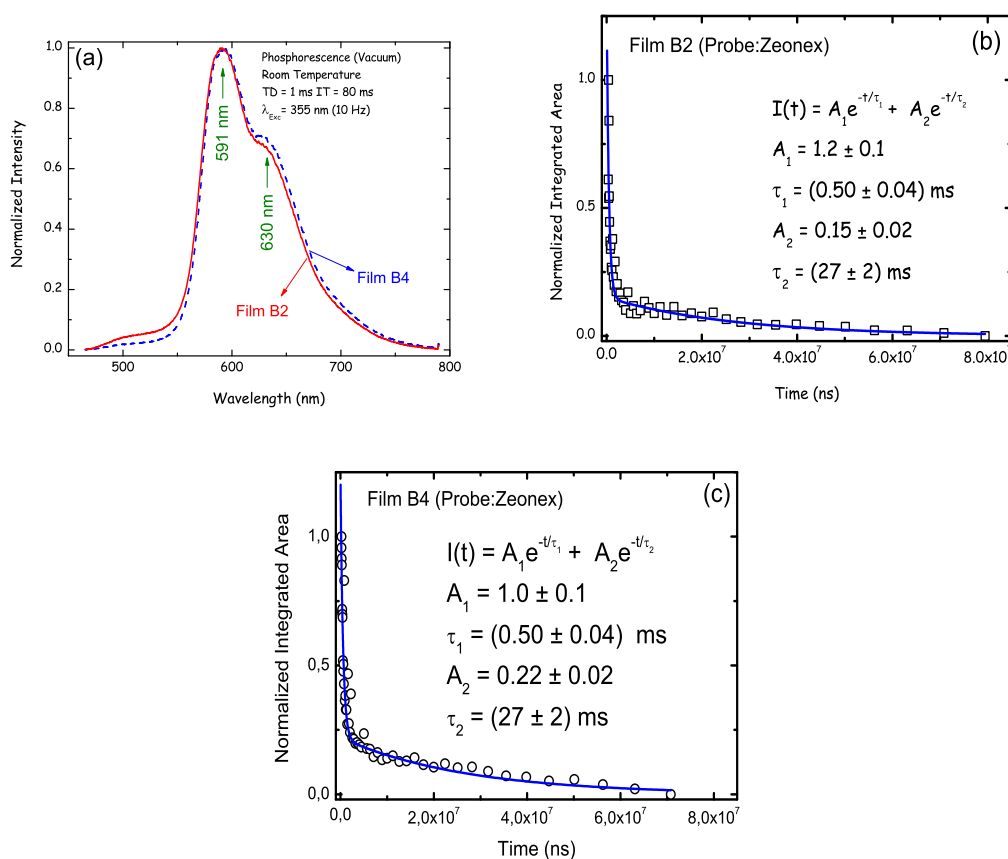


FIG. 5: (Color Online) (a) Normalized Phosphorescence (PH) spectra obtained from gated fluorescence for the B_2 and B_4 films using $TD = 1$ ms and $IT = 80$ ms; (b) and (c) are respectively the PH Decay curves of the B_2 (squares) and B_4 (circles) films obtained by gated fluorescence. The corresponding lifetime components ($\tau_i, i = 1, 2$), obtained from the fitting of the respective decay data (dashed lines), are shown in the respective inset. The measurements of PH spectra in (a) and the PH decays in (b) and (c) were performed at room temperature, under vacuum, with the excitation made by a 355 nm pulsed laser line (repetition rate of 10 Hz).

times for the B_2 film of $\tau_1 = 0.50$ ms and $\tau_2 = 27$ ms. The weight contributions for the overall emission were $W_1 = 0.13$ and $W_2 = 0.87$, respectively. The same τ_1 and τ_2 lifetimes were obtained for the film B_4 , with slightly different weights $W_1 = 0.08$ and $W_2 = 0.92$. Although bi-exponential profiles of B_2 and B_4 films could indicate contributions from the monomer and dimer character, as considered for the singlet decays, the similarities of lifetimes, the weight contributions and even though the PH spectra between them (Fig. 5a) do not enable us to infer directly on the consequences of dimer formation on triplet states. The most important experimental aspect that could be related to the aggregation effects on triplet states is the decrease of the PH yield at steady-state conditions, decreasing from $\phi = (4.1 \pm 1.0)\%$ in film B_2 to $\phi = (1.0 \pm 0.2)\%$ in film B_4 , as we reported before.⁵ The higher yield measured for film B_2 means that lower level of intermolecular interaction and, therefore, lower influence of aggregate states promotes higher luminescence efficiency. In turn, lower yield measured for film B_4 would

be consistent with the possibility of TTA events in this most concentrated film.

When Zeonex[®] is removed (consistent with a less rigid medium) the PH of phenazine-based 1,2,3-triazole molecules in neat films is not observed. This is clearly due to a more effective vibrational quenching of the triplet population. On the other hand, delayed fluorescence (DF) was clearly observed with maximum intensity around 540 nm, *i.e.* in the aggregate form, corresponding to very long-lived singlet aggregate states, which are probably formed as a result of TTA, occurring in dimers due to better triplet mobility in neat films. It is worth mentioning that these DF spectra (Figs. 4a and 4b) are relatively noisy compared to the PH signal obtained at the same TD and IT conditions (Fig. 5a).

The detection of the DF spectra around 540 nm at $TD = 1$ ms, instead of PH spectra, is the experimental proof of the change of the dynamics of the probe neat films when compared to the blended films B_2 and B_4 . This indicates that the emission dynamics is strongly de-

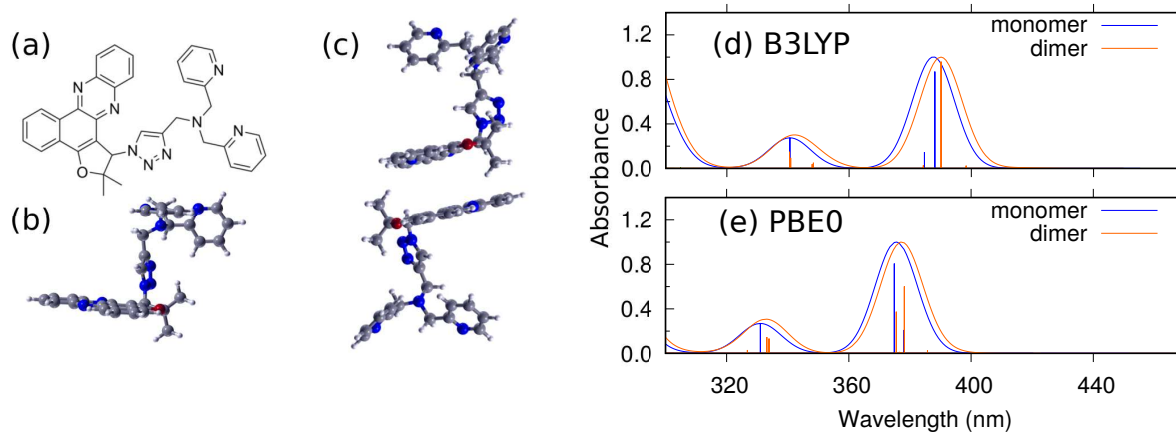


FIG. 6: (Color Online) (a) Schematic view of the monomer structure of the probe derivative phenazine molecule. In (b) and (c) are shown the optimized geometries of the monomer and dimer, respectively. In (d) and (e) are the normalized UV-Vis absorption spectra of the monomer and dimer calculated with B3LYP and PBE0 functionals, respectively.

pendent on the intermolecular interactions and/or the conformational properties of the molecular system,^{18–20} demonstrating a more detrimental effect for the emission of triplet states in neat films.

In order to investigate the structure of the aggregate form in the phenazine-based 1,2,3-triazole molecules, computational studies were performed using the density functional theory (DFT) and its time-dependent formalism (TD-DFT) as implemented as in the ORCA code version 4.0.0.²¹ The hybrid exchange correlation B3LYP functional^{22–24} with a def2-SVP²⁵ basis set was used to obtain the optimized geometries of the monomer and aggregated forms. The results clearly reveal the formation of dimer states is favoured in the phenazine-based 1,2,3-triazole molecule studied here, forming a quasi-parallel sandwich type arrangement between the two phenazines.

TD-DFT calculations were also carried out to find the electronic levels involved in the excitations and to calculate the monomer and aggregate UV-Vis spectra. Furthermore, the UV-Vis spectra were obtained with two different exchange correlation hybrid functionals: B3LYP and PBE0.²⁶ For PBE0 we used the fixed geometries obtained with B3LYP functional. In all TD-DFT calculations, the first 20 singlet excited states were calculated with a tight criteria for the convergence of the self-consistent field (SCF) iteration. To provide a simple visualization of the UV-Vis spectra, the TD-DFT excitation energies and oscillator strengths were convoluted with normalized Gaussian functions with a 8 nm full width at half maximum.

Figure 6a shows a planar schematic view of the monomer, featuring a phenazine group bonded to a N,N-bis(pyridin-2-ylmethyl)prop-2-yn-1-amine.¹⁶ The optimized geometry in Fig. 6b reveals its three dimensional structure, exhibiting the planar configuration of the phenazine group. The dimer was constructed by the stacking of such planar regions. Two initial con-

figurations were considered, and both converged to the same optimized geometry shown in Fig. 6c. The theoretical UV-Vis spectra shown in Figs. 6d and 6e, despite the simple models used, are qualitatively valid for comparison purposes. For the monomer and dimer, both functionals employed led to similar UV-Vis, except for an overall violet shift in the PBE0 case relative to the B3LYP result. For the monomer, two intense electronic transitions are observed in the range of 360.0 and 400.0 nm, the most intense peak observed at 388.1 nm and at 374.9 nm in the B3LYP and PBE0 calculations, respectively. As it can be seen in Table S1 of the supplementary material, these intense peaks may be ascribed to transitions from the HOMO-1 to LUMO, and these two orbitals are localized in the planar phenazine compound (Fig. S2 of the supplementary material). The less intense peaks correspond to transitions from lower states to the LUMO (Table S1 of the supplementary material). Regarding the dimer UV-Vis spectra, several electronic transitions in the range of 360.0 and 400.0 nm with vanishing oscillator strengths were identified, and the most intense electronic transitions in this range have contributions from excitations between molecular orbitals in the planar phenazine group (see Table S2 and Fig. S3 of the supplementary material). Furthermore, both functionals reveal a red shift in the UV-Vis spectra of the dimer in relation to the spectra of the monomer. This effect may be related to the modification of the molecular orbitals in the planar phenazine compound when the dimer is formed, lowering the energy of the orbitals and, consequently, lowering the energy of the electronic transitions. The red shift obtained with both functionals after the dimerisation is in qualitative good agreement with the experimental results. In fact, the UV-Vis spectrum for the B₄ film (Fig. 1), which is the most likely to form dimers, clearly suggests the existence of states shifted towards larger wavelengths (broadening effect).

IV. CONCLUSIONS

Dropcast blended films B_2 and B_4 , produced from phenazine derivative solutions of low and high concentrations respectively mixed with Zeonex[®] matrix, were investigated by time-resolved luminescence spectroscopy at room temperature. TRFL emissions around 430 nm and 540 nm, were observed at different time delays, and assigned as coming from monomer and dimer species, respectively in the film B_2 , while for the film B_4 only the dimer TRFL emission was observed. These results put in evidence the consequences of aggregation effects on the singlet emission dynamics of organic materials

No direct aggregation effects were observed on the lifetime of the triplet state, measured by the PH emission decay from films B_2 and B_4 , or the shape of their PH spectra. The PH emissions at steady state conditions, however, were observed to be more intense than the fluorescence ones, even though at room temperature.⁵ The QY of the film B_2 was also observed to be relatively higher than that of the film B_4 . The dimer formation in film B_2 it is not so predominant as it is in film B_4 . These experimental facts indicate that aggregation effects are detrimental to the emission of triplet states in organic materials.

Going further in the research of aggregation effects on the dynamics of singlet and triplet emissions we investigated neat films of derivative phenazine probe molecules. These films present higher intermolecular interaction, *i.e.*, higher aggregation effect is expected due to the absence of the Zeonex[®] matrix. However, effective electron interactions with molecular vibrational modes are enhanced, strongly favoring non-radiative emission decay. For the singlet states, increasing intermolecular interactions leads to weaker emission. This was experimentally observed for the neat films, where just singlet TRFL monomer emissions have survived at early times, independently of their low or high probe molecule concentration. For the emission taken at relatively long time delay ($TD = 1$ ms), both neat films (low and high concentra-

tions) presented a delayed and relatively weak emission due to dimer states (centered around 540 nm) instead of the expected PH emission. Considering the competing character between PH emissions with non-radiative decays due to vibrations and/or TTA, the PH is effectively quenched, as observed experimentally, due to the much higher probability of non-radiative recombination processes at room temperature in neat films.

In summary, the strong dependence of the emission dynamics of singlet and triplet states of phenazine derivatives on molecular aggregation was demonstrated in this work. The different preparation conditions of the films leads to the observation of relatively large PLQY and relatively strong room temperature phosphorescence in the more viscous films containing Zeonex[®]. In other words, films with the minimum contribution of aggregates must present enhanced photophysical properties with much lower TTA and non-radiative losses. Thus, the higher dilution of the probe molecule in Zeonex[®], as used in film B_2 , was essential to achieve these conditions. The results presented here have a direct importance concerning potential applications, in particular, purely organic phosphorescent light emitting diodes.

V. CONFLICTS OF INTEREST

There are no conflicts of interest to declare.

Acknowledgments

L. A. Cury, G. A. M. Jardim, E. N. da Silva Jr., O. J. Silveira and M. J. S. Matos thank FAPEMIG, CAPES and CNPq from Brazil for the financial support. P. L. dos Santos thanks CAPES - Science Without Borders, Brazil, for the Doctorate studentship, Proc. 12027/13-8. The authors also acknowledge Dr. Mário S. C. Mazzoni for fruitful discussions on the TD-DFT calculations.

¹ M. Más-Montoya, R. A. J. Janssen, *Adv. Funct. Mater.* **27**, 1605779 (1-12) (2017).

² S. Reineke, M. A. Baldo, *Scientific Reports* **4**, 3797 (2014).

³ N. Kleinhenz, N. Persson, Z. Xue, P. H. Chu, G. Wang, Z. Yuan, M. A. McBride, D. Choi, M. A. Grover, E. Reichmanis, *Chem. Mater.* **28**, 3905 (2016).

⁴ S. D. Spencer, C. Bougher, P. J. Heaphy, V. M. Murcia, C. P. Gallivan, A. Monfette, J. D. Andersen, J. A. Cody, B. R. Conrad, C. J. Collison, *Solar Energy Materials & Solar Cells* **112**, 202 (2013).

⁵ B. B. A. Costa, P. D. C. Souza, R. N. Gontijo, G. A. M. Jardim, R. L. Moreira, E. N. da Silva Júnior, Luiz A. Cury, *Chem. Phys. Lett.* **695**, 176 (2018).

⁶ K. Hany, X. Luy, J. Xuy, G. Zhouy, S. May, W. Wangy, Z. Caiz, J. Zhouz, *J. Phys. D: Appl. Phys.* **30**, 2923 (1997).

⁷ P. L. dos Santos, J. S. Ward, A. S. Batsanov, M. R. Bryce, A. P. Monkman, *The Journal of Physical Chemistry C* **121**, 16462 (2017).

⁸ D. Lee, O. Bolton, B. C. Kim, J. H. Youk, S. Takayama, J. Kim, *J. Am. Chem. Soc.* **135**, 6325 (2013).

⁹ S. Mukherjee, P. Thilagar, *Chem. Commun.* **51**, 10988 (2015).

¹⁰ B. B. A. Costa, G. A. M. Jardim, P. L. Santos, H. D. R. Calado, A. P. Monkman, F. B. Dias, E. N. da Silva Júnior, L. A. Cury, *Phys. Chem. Chem. Phys.* **19**, 3473 (2017).

¹¹ Y. Hirata, I. Tanaka, *Chem. Phys. Lett.* **43**, 568 (1976).

¹² A. Grabowska, *Chem. Phys. Lett.* **1**, 113 (1967).

¹³ T. G. Pavlopoulos, *Spectrochim. Acta* **43A**, 715 (1987).

¹⁴ J. I. DelBarrio, J. R. Rebato, F. M. G. Tablas, *J. Phys. Chem.* **93**, 6836 (1989).

- ¹⁵ V. A. Kuz'min, P. P. Levin, *Bull. Acad. Sci. USSR Div. Chem. Sci.* 37, 1098 (1988).
- ¹⁶ G. A. M. Jardim, H. D. R. Calado, L. A. Cury, E. N. da Silva Júnior, *Eur. J. Org. Chem.* 2015, 703 (2015).
- ¹⁷ B. B. A. Costa, P. L. Santos, M. D. R. Silva, S. L. Nogueira, K. A. S. Araujo, B. R. A. Neves, T. Jarrosson, F. Serein-Spirau, J.-P. Lére-Porte, L. A. Cury, *Chem. Phys. Lett.* 614, 67 (2014).
- ¹⁸ H. H. Billsten, V. Sundström, T. Polívka, *J. Phys. Chem. A* 109, 1521 (2005).
- ¹⁹ H. H. Billsten, D. Zigmantas, V. Sundström, T. Polívka, *Chem. Phys. Lett.* 355, 465 (2002).
- ²⁰ M. Durchan, M. Fuciman, V. Šlouf, G. Kesan, T. Polivka, *J. Phys. Chem. A* 116, 12330 (2012).
- ²¹ F. Neese, *WIREs Comput. Mol. Sci.* 2, 73 (2012).
- ²² A. D. Becke, *Phys. Rev. A* 38, 3098 (1988).
- ²³ C. Lee, W. Yang, R. G. Parr, *Phys. Rev. B* 37, 785 (1988).
- ²⁴ A. D. Becke, *J. Chem. Phys.* 98, 5648 (1993).
- ²⁵ A. Schafer, H. Horn, R. Ahlrichs, *J. Chem. Phys.* 97, 2571 (1992).
- ²⁶ C. Adamo, V. Barone, *J. Chem. Phys.* 110, 6158 (1999).

Dynamics of aggregated states resolved by gated fluorescence in films of room temperature phosphorescent emitters

Paloma L. dos Santos^{1‡}, Orlando J. Silveira², Rongjuan Huang¹, Guilherme A. M. Jardim³, Matheus J. S. Matos⁴, Eufrânio N. da Silva Júnior³, Andrew P. Monkman¹, Fernando B. Dias¹, Luiz A. Cury^{2†}

¹*Department of Physics, University of Durham, South Road DH1 3LE, Durham, United Kingdom*

²*Instituto de Ciências Exatas, Departamento de Física, Universidade Federal de Minas Gerais, 31270-901, Belo Horizonte, Minas Gerais, Brazil*

³*Instituto de Ciências Exatas, Departamento de Química, Universidade Federal de Minas Gerais, 31270-901, Belo Horizonte, Minas Gerais, Brazil*

⁴*Instituto de Ciências Exatas e Biológicas, Departamento de Física, Universidade Federal de Ouro Preto, 35400-000, Ouro Preto, Minas Gerais, Brazil*

(Dated: January 15, 2019)

Phenazine derivative molecules were studied using steady state and time resolved fluorescence techniques and demonstrated to lead to strong formation of aggregated species, identified as dimers by time dependent density functional theory calculations. Blended films in a matrix of Zeonex[®], produced at different concentrations, showed different contributions of dimer and monomer emissions in the prompt time frame, e.g. less than 50 ns. In contrast, the phosphorescence (e.g. emission from the triplet state) shows no significant effect on dimer formation, although strong dependence of the phosphorescence intensity on concentration is observed, leading to phosphorescence being quenched at higher concentration.

I. INTRODUCTION

The study of molecular photophysics in solid films has gained strong interest over the past 20 years due to their relevance for the performance of many devices in the molecular optoelectronics field, such as organic light emitting diodes (OLEDs). The luminescence properties of thin films of organic molecules, however, require extensive characterization, since film morphology, molecular structure, packing conditions and the presence of aggregated species, among other effects, have strong influence on the optical and charge transport properties of organic compounds.^{1–7} In the particular area of OLEDs, the improvement of luminescence yields and triplet harvesting properties is key to boost devices performance. For example, improving the OLEDs efficiency is often attempted by trying to maintain strong luminescence yields, while trying to facilitate triplet states to contribute to the production of electroluminescence. Heavy-metal complexes are a class of materials with potential to solve this dilemma, by exploring the strong spin-orbit coupling created by the presence of the heavy-atom leading to emission directly from the triplet state. However, while successful these materials are also prone significant degradation in the blue region, and may create environmental problems when used in high-production output technologies, such as displays and lighting. Metal-free compounds are thus very attractive for application in OLEDs, subsequently they are able to harvest triplet

states and show sufficient strong luminescence yield in solid state.

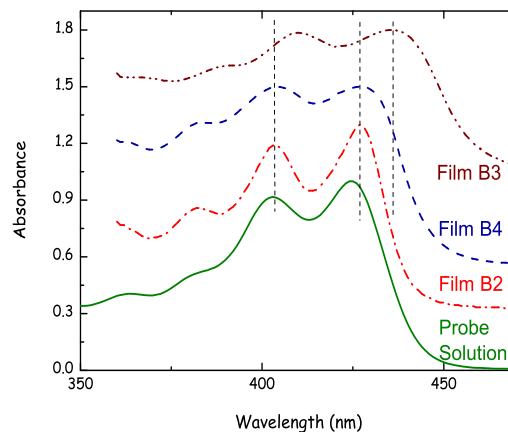


FIG. 1: (Color Online) The normalized UV-Vis absorption spectra for the neat film B_3 (dashed-dotted-dotted line), for the probe:Zeonex[®] blended film B_4 (dashed line), for the probe:Zeonex[®] blended film B_2 (dashed-dotted line), and for the solution of the probe molecule at 0.1 mg/mL in $CHCl_3$ (solid line), at room temperature. The spectra were displaced from each other for clarity sake.

Thermally activated delayed fluorescence reemerged recently as a successful way to promote triplet harvesting (TADF) in metal-free organic compounds. In OLEDs using TADF's the 75% triplet states that are created upon charge recombination are up-converted to the singlet manifold via thermally-activated reverse intersystem crossing. This mechanism gives origin to delayed fluores-

[‡]1st corresponding author. Paloma Lays dos Santos (p.l.dos-santos@durham.ac.uk)

[†]2nd corresponding author. Luiz Alberto Cury (cury@fisica.ufmg.br)

cence, allowing the device internal quantum efficiency to increase up to 100%, in contrast with the maximum 25% that would be otherwise obtained.

Related with the TADF mechanism, the possibility of obtaining direct room temperature phosphorescence (RTP) from metal-free organic compounds has also promoted strong interest in many applications, such as imaging, oxygen sensing, anti-counterfeit labelling, and even OLEDs. Strong RTP is difficult to achieve in metal-free compounds due to the spin forbidden character of phosphorescence, which makes the triplet excited state likely to suffer non-radiative deactivation caused by vibrations and energy transfer to oxygen, among other quenching processes. RTP emitters, therefore, should have high triplet formation yield, which is usually accomplished by the inclusion of heteroatoms in the molecular structure. Nitrogen and Sulphur in particular are effective in creating strong spin-orbit interactions involving $n\pi^*$ transitions, in conformity with El-Sayed's rule. Besides strong triplet formation yields, the observation of strong RTP requires also weak vibrational luminescence quenching. This is mostly accomplished using the influence of intermolecular interactions in crystals and aggregates. However, there are also examples where RTP has been observed in single molecules in isolation, when dispersed in suitable host, such as PMMA or Zeonex[®].^{8,9} In contrast, the observation of RTP from metal-free compounds in liquid phase is extremely rare and intriguing. We are aware of just a few cases, including the case of a phenazine derivative reported recently in our groups.^{5,10} This clearly shows that a systematic understanding of structure-property relationships to create RTP emitters is still lacking.

In this work we report the steady state and time resolved optical spectroscopy studies on a phenazine-based 1,2,3-triazole probe molecule, which shows strong room temperature phosphorescence.¹⁰⁻¹⁵ Samples showing different levels of intermolecular interactions were studied in solution and solid state (neat and blended films using Zeonex[®] host), seeking to unravel the role of aggregate species on the origin of RTP in this phenazine derivative. The results enabled us to observe the presence of different species emitting from their singlet state, with different time resolved fluorescence (TRFL) forms appearing at different delay times, and corresponding to distinct singlet state fluorescence decays. Time dependent density functional theory (TD-DFT) was also employed and the absorption spectra of the monomer and aggregate (dimer) species of the probe molecule were calculated. The comparison of the theoretical and experimental absorption bands strongly indicates that the formation of molecular dimers are the origin of the distinct fluorescence spectra.

Differently from TRFL very similar phosphorescence (PH) spectra and decays were observed for the blended films at different concentrations, therefore, revealing that in contrast with the singlet emission the triplet state is much less affected by the formation of dimers. The

larger difference in this sense was perceived by the decrease of the phosphorescence quantum yield (QY) for the higher concentration sample, revealing a quenching effect on phosphorescence due to concentration.

II. SAMPLES AND EXPERIMENTAL DETAILS

The available natural lapachol compound, extracted from the heartwood of *Tabebuia sp.* (Tecoma) has been used to synthesized the phenazine-based 1,2,3-triazole luminescent and phosphorescent probe molecule investigated in this work. The synthetic route of this derivative phenazine molecule is described in details in the literature.¹⁶

Dropcast films, B_2 and B_4 , were produced respectively from two Probe:Zeonex[®] blend chloroform ($CHCl_3$) solutions, S_2 and S_4 , deposited on glass substrates at room temperature. The blend solution S_2 was prepared adding 366 mg of Zeonex[®] into 5 mL of a probe solution in $CHCl_3$ with 0.1 mg/mL concentration. The blend solution S_4 was prepared adding 1 mL of a probe solution with 3.0 mg/mL concentration in $CHCl_3$ to 4 mL of a Zeonex[®] $CHCl_3$ solution with 71 mg/mL concentration. Considering just the amount of the probe molecule in $CHCl_3$ volume, the final concentrations for the solutions S_2 and S_4 are respectively 0.1 mg/mL and 0.6 mg/mL. Both solutions were left stirring for at 24 h. The Zeonex[®] cyclo-olefin polymers (ZEON Corporation) is an optically inert matrix used to disperse the probe molecules. After drying the solvent, the Zeonex[®] matrix provides a strong rigid medium for the probe molecules in the films. TRFL and PH spectra for the B_2 and B_4 films, obtained in vacuum (10^{-4} Torr) and at room temperature, were recorded using nanosecond and millisecond gated fluorescence acquisition. The excitation source was a high-energy pulsed Nd:YAG laser emitting at 355 nm (EKSPILA). Emissions were focused onto a spectrograph and detected on a sensitive gated iCCD camera (Stanford Computer Optics) having sub-nanosecond resolution. TRFL and PH time resolved measurements were performed by increasing integration and delay times. TRFL decays for the films B_2 and B_4 were also collected using the picosecond time correlated single photon counting (TCSPC) technique (instrument response function 24 ps). In this case, the films were excited by a second harmonic pulse ($\lambda = 394$ nm, 76 MHz of repetition rate) from a mode-locked Ti:sapphire laser from Coherent Inc., with vertical polarization. The emission was detected through a double-subtractive monochromator (SpectraPro-2300i), and a MCP detector (Hamamatsu model R3809U-50) was used to collect decays at different wavelengths. UV-Vis absorption measurements of the blended films B_2 , B_4 , the neat film B_3 , and for a reference probe solution in $CHCl_3$, at relatively low concentration (0.1 mg/mL), were performed at room temperature in a spectrophotometer Shimadzu, model 3600. The drop-casting neat film B_3 on glass substrate, made from

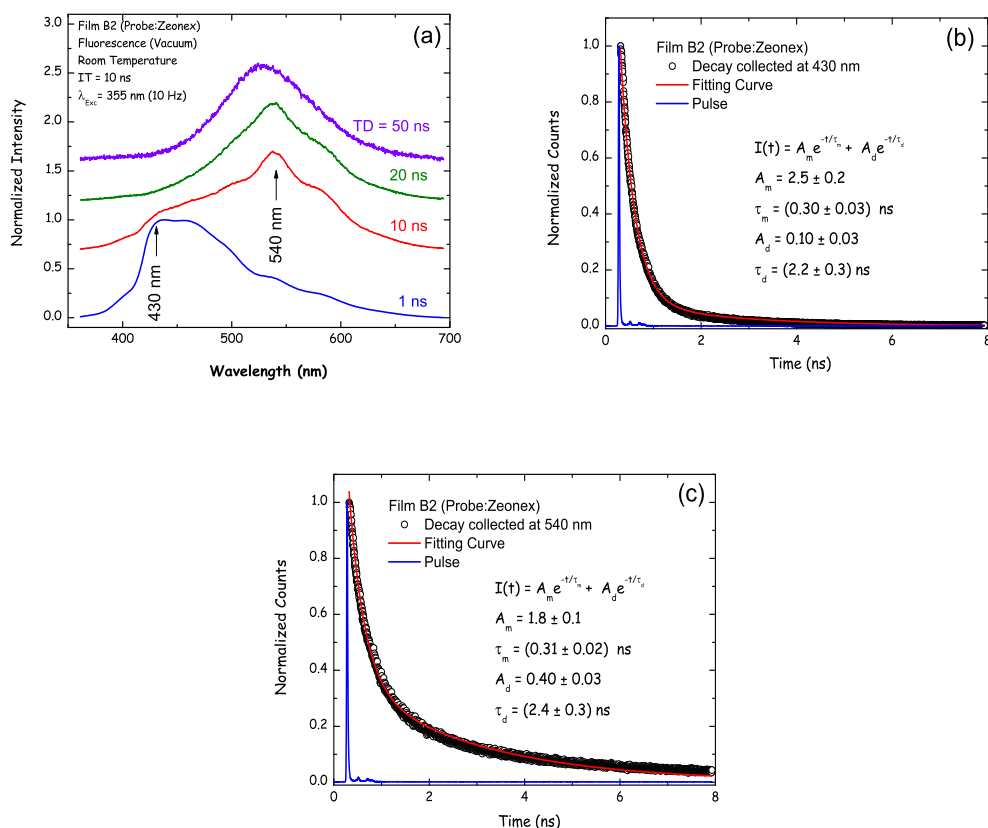


FIG. 2: (Color Online) (a) Time resolved fluorescence (TRFL) spectra obtained for the film B_2 at time delays (TDs) of 1 ns, 10 ns, 20 ns and 50 ns. The TRFL measurements were performed at room temperature, under vacuum, with the excitation made by a 355 nm pulsed laser line (repetition rate of 10 Hz). The spectra were normalized and displaced from each other for clarity sake. The integration time (IT) of 10 ns was used in all measurements; (b) Time correlated single photon counting (TCSPC) decay obtained for the film B_2 with emission collected at 430 nm; (c) TCSPC decay obtained for the film B_2 with emission collected at 540 nm. The TCSPC decays were obtained with the excitation made by a second harmonic pulsed laser ($\lambda = 394$ nm, 76 MHz of repetition rate) from a mode-locked Ti:sapphire laser, Coherent Inc.. The corresponding lifetime components (τ_m and τ_d), obtained by fitting the decay data (solid lines) in (b) and (c), are shown in the respective insets. Deconvolution process of the decays in parts (b) and (c) were not considered due to the relatively low instrument response function (IRF) of the TCSPC system (24 ps). The pulse curves in (b) and (c), representing the IRF, are shown just for the completeness sake.

a probe solution at 3.0 mg/mL in $CHCl_3$, was measured for the sake of aggregation effect comparison.

III. RESULTS AND DISCUSSIONS

Figure 1 shows the normalized absorption spectra of phenazine-based 1,2,3-triazole molecules in solution and solid state. The comparison among these spectra indicates the presence of aggregates in the films, as suggested by the slight red shift observed from solution to blended Zeonex[®] films (weak aggregation effect) and further in neat film (strong aggregation effect). The red shift is probably due to the presence of relatively longer conjugated regions in the molecular aggregates, when com-

pared with the single molecules.^{5,17} Importantly, as the effect of aggregation is observed in the absorption it is therefore associated with the grounded state, rather than formation of excimers, which occurs just in the excited state, and shows no signature in absorption spectra. It is also important to notice in **Fig. 1** that for the stronger aggregation effect observed for the neat film B_3 , beyond the effective redshift, a clear broadening of the absorption bands occurs, which is also observed for the blended film B_4 (high concentration) but relatively less for the film B_2 (low concentration), as expected due to its weaker character of aggregation. **Figure S1a** in the supplementary materials shows the absorption spectra of phenazine-based 1,2,3-triazole molecules in solution at relatively lower concentrations just for comparison.

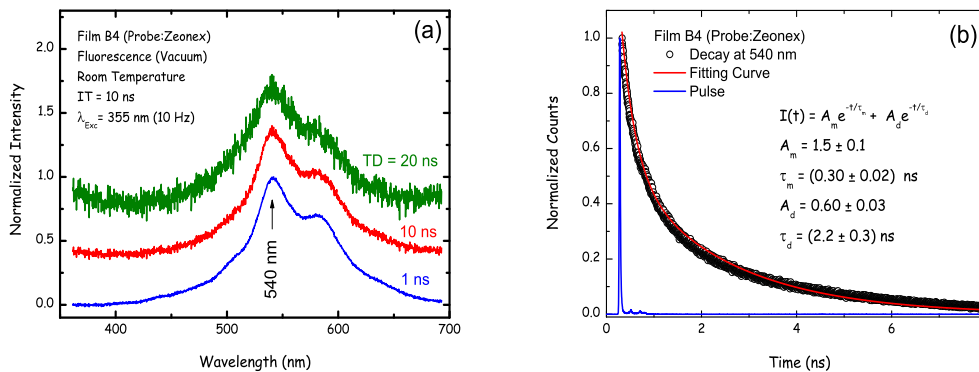


FIG. 3: (Color Online) (a) TRFL spectra obtained for the film B_4 at time delays (TD) of 1 ns, 10 ns, and 20 ns. The TRFL measurements were performed at room temperature, under vacuum, with the excitation made by a 355 nm pulsed laser line (repetition rate of 10 Hz). The spectra were normalized and displaced from each other for clarity sake. The integration time (IT) of 10 ns was used in all measurements; (b) Time correlated single photon counting (TCSPC) decay obtained for the film B_4 at 540 nm. The TCSPC decay was obtained with the excitation made by a second harmonic pulsed laser ($\lambda = 394$ nm, 76 MHz of repetition rate) from a mode-locked Ti:sapphire laser, Coherent Inc.. The corresponding lifetime components (τ_m and τ_d), obtained by fitting the decay data (solid line), are shown in the inset. Deconvolution process of the decay in part (b) was not considered due to the relatively low instrument response function (IRF) of the TCSPC system (24 ps). The pulse curve in (b), representing the IRF, is shown just for the completeness sake.

Film	Monomer			Dimer		
	A_m	τ_m (ns)	W_m	A_d	τ_d (ns)	W_d
B_2 at 430 nm	(2.5 ± 0.2)	(0.30 ± 0.03)	0.77	(0.10 ± 0.03)	(2.2 ± 0.3)	0.23
B_2 at 540 nm	(1.8 ± 0.1)	(0.31 ± 0.02)	0.37	(0.40 ± 0.03)	(2.4 ± 0.3)	0.63
B_4 at 540 nm	(1.5 ± 0.1)	(0.30 ± 0.02)	0.25	(0.60 ± 0.03)	(2.2 ± 0.3)	0.75

TABLE I: Pre-exponential factors A_m and A_d , the corresponding lifetimes τ_m and τ_d , and the corresponding weights W_m and W_d for monomer and dimer contributions obtained from the decay curves (Figs. 2 and 3) at room temperature for the films B_2 and B_4 , respectively. The weights are calculated by $W_m = A_m \tau_m / [A_m \tau_m + A_d \tau_d]$ and $W_d = A_d \tau_d / [A_m \tau_m + A_d \tau_d]$.

To further investigate the formation of aggregates in phenazine-based 1,2,3-triazole films, time resolved emission spectra in the nanosecond time frame were obtained. The TRFL spectra at different time delays (TDs) for film B_2 (0.1 mg/ml phenazine-based 1,2,3-triazole in Zeonex[®]) are shown in Fig. 2a.

The TRFL spectrum at $TD = 1$ ns (Fig. 2a) shows an emission spectrum with a maximum intensity at 430 nm. The steady-state photoluminescence spectra for probe solutions in $CHCl_3$ at relatively lower concentrations, shown in Fig. S1b in the supplementary materials, are representatives of a more monomeric character of the probe emission. The difference for the peak emission, around 450 nm for lower concentration solutions and that at 430 nm for film B_2 is a consequence of different conformational molecular states. Thus, the emission in film B_2 is therefore, mostly assigned to the monomeric form of phenazine-based 1,2,3-triazole. However, a shoulder around 540 nm is also observed, showing that the emission at 1 ns is not purely from the monomer species.

With increasing time delay, the TRFL spectra consecutively changes shape, showing clear displacement from blue to the green region with time (peak around 540 nm), but still presenting a weak shoulder around 430 nm. Finally, at later times ($TD = 50$ ns) the predominant emission shows a Gaussian-type emission peaking around 540 nm, and no shoulder at 430 nm is observed. The film B_2 is formed by a relatively low concentration of phenazine-based 1,2,3-triazole molecules, randomly dispersed in the Zeonex[®] matrix. In these conditions, both monomer and aggregated (dimer) forms can be observed. Their corresponding energies are between the singlet [$E_{PL} = (2.88 \pm 0.02)$ eV (≈ 430 nm)] and triplet [$E_{PH} = (2.19 \pm 0.08)$ eV (≈ 566 nm)] energies, obtained from the onset lines of steady-state emission spectrum of film B_2 at 79 K, as shown in Fig. S2 in the supplementary materials.

The TCSPC decay collected at 430 nm and 540 nm for the film B_2 , are shown, respectively, in Figs. 2b and 2c. The decay at 430 nm shows two clear pre-exponential

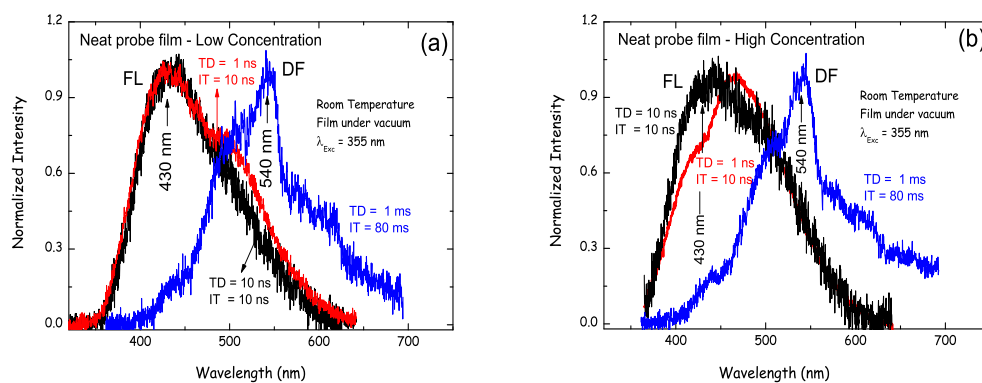


FIG. 4: (Color Online) (a) Normalized time resolved fluorescence (TRFL) spectra of the probe neat film made from the low concentration (0.1 mg/mL) probe solution at $TD = 1 \text{ ns}$ and 10 ns with $IT = 10 \text{ ns}$, and the delayed fluorescence (DF) spectrum at $TD = 1 \text{ ms}$ and $IT = 80 \text{ ms}$; (b) Normalized TRFL spectra of the probe neat film made from the high concentration (3.4 mg/mL) probe solution at $TD = 1 \text{ ns}$ and 10 ns with $IT = 10 \text{ ns}$, and the DF spectrum at $TD = 1 \text{ ms}$ and $IT = 80 \text{ ms}$. The measurements of TRFL and DF spectra in (a) and in (b) were performed at room temperature, under vacuum, with the excitation made by a 355 nm pulsed laser line (repetition rate of 10 Hz).

components (A_m and A_d) and is, therefore, associated with two distinct lifetimes, $\tau_m = (0.30 \pm 0.03) \text{ ns}$ and $\tau_d = (2.2 \pm 0.3) \text{ ns}$, with contribution weights to the overall emission of $W_m = 0.77$ and $W_d = 0.23$, respectively. The faster decay component (τ_m) is associated with the monomer emission, and contributes with most of emission collected at 430 nm , as expected. The longer lifetime (τ_d) is thus associated with the dimer species and dominates the decay collected at 540 nm . This emission also shows bi-exponential decay, $\tau_m = (0.31 \pm 0.02) \text{ ns}$ ($W_m = 0.37$) and $\tau_d = (2.4 \pm 0.3) \text{ ns}$ ($W_d = 0.63$), but with relatively stronger weight of the long-lived decay component.

For the film B_4 , with the higher concentration, and thus, higher degree of intermolecular interaction between phenazine-based 1,2,3-triazole molecules, the TRFL spectrum obtained at initial delay time, $TD = 1 \text{ ns}$, (Fig. 3a), shows the maximum emission intensity position already displaced to the green region, peaking at 540 nm . With increasing time delay, the shape of the TRFL spectra remains practically unchanged. The TRFL corresponding to the dimer form is thus predominant since early times in the B_4 film. This is also strongly supported by the increased contribution of the longer decay component (τ_d), which now represents a weight $W_d = 0.75$ of the overall emission (Fig. 3b). Table 1 shows the pre-exponential factors, the lifetimes, and weights, associated to each exponential (monomer and dimer) for both blended films B_2 and B_4 , highlighting the contributions of monomer and dimer in each sample.

Figures 4a and 4b show the TRFL emission spectra for neat films made from low (0.1 mg/mL) and high (3.4 mg/mL) concentration probe solutions. In both cases the aggregated form would be pre-

dominant due to the absence of Zeonex[®] host. Surprisingly, the emissions collected at early time delays ($TD = 1 \text{ ns}$ and 10 ns) in both, show predominance of monomer emission, with intensity peaking around 430 nm , and only at late time ($TD = 1 \text{ ms}$) the emissions from aggregates around 540 nm are observed. It is well known that Zeonex[®] is very effective on suppressing molecular vibrations, which makes it a very effective host for observation of RTP.⁵ However, in the absence of Zeonex[®] molecular vibrations may contribute for aggregate dissociation making the monomer form dominant in neat films. The overall emission observed in these neat films are very weak compared to the blended probe:Zeonex[®] films (Figs. 2a and 3a). This is a result of the strong emission quenching of the excited states by the packing conditions in neat films, where non-radiative vibrational mode emissions take place effectively. Consequently, the corresponding PLQYs at steady-state conditions of the neat films are observed to be relatively lower than those of blended probe:Zeonex[®] films, as reported before.⁵

The room temperature phosphorescence spectra of phenazine-based 1,2,3-triazole dispersed in Zeonex[®] at two different concentrations (blended films B_2 and B_4) are shown in Fig. 5a. Strong RTP emission is observed as Zeonex[®] is very effective on suppressing vibrations, allowing PH to compete with non-radiative decay processes that may quench the triplet excited state population. It is also worth mentioning that the PH dominates the steady-state emission, even at room temperature, in both B_2 and B_4 films. Moreover, Zeonex[®] also separates phenazine-based 1,2,3-triazole molecules, minimizing the occurrence of triplet-triplet annihilation (TTA), which would also compete against the PH emission.

The PH decays for both B_2 and B_4 films show bi-exponential profiles (see Figs. 5b and 5c), with decay

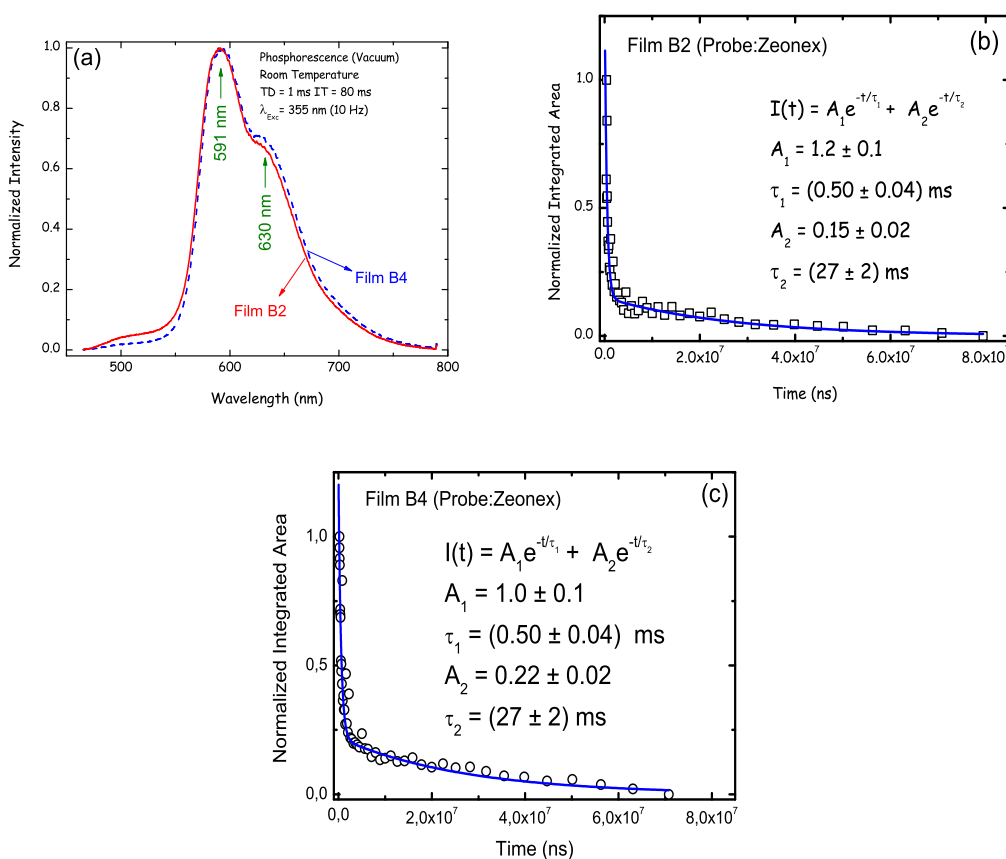


FIG. 5: (Color Online) (a) Normalized Phosphorescence (PH) spectra obtained from gated fluorescence for the B_2 and B_4 films using $TD = 1$ ms and $IT = 80$ ms; (b) and (c) are respectively the PH decay curves of the B_2 (squares) and B_4 (circles) films obtained by gated fluorescence. The corresponding lifetime components ($\tau_i, i = 1, 2$), obtained from the fitting of the respective decay data (dashed lines), are shown in the respective inset. The measurements of PH spectra in (a) and the PH decays in (b) and (c) were performed at room temperature, under vacuum, with the excitation made by a 355 nm pulsed laser line (repetition rate of 10 Hz).

times for the B_2 film of $\tau_1 = 0.50$ ms and $\tau_2 = 27$ ms. The weight contributions for the overall emission were $W_1 = 0.13$ and $W_2 = 0.87$, respectively. The same τ_1 and τ_2 lifetimes were obtained for the film B_4 , with slightly different weights $W_1 = 0.08$ and $W_2 = 0.92$. Although bi-exponential profiles of B_2 and B_4 films could indicate contributions from the monomer and dimer character, as considered for the singlet decays, the similarities of lifetimes, the weight contributions and even though the PH spectra between them (Fig. 5a) do not enable us to infer directly on the consequences of dimer formation on triplet states. The most important experimental aspect that could be related to the aggregation effects on triplet states is the decrease of the PH yield at steady-state conditions, decreasing from $\phi = (4.1 \pm 1.0)\%$ in film B_2 to $\phi = (1.0 \pm 0.2)\%$ in film B_4 , as we reported before.⁵ The higher yield measured for film B_2 means that lower level of intermolecular interaction and, therefore, lower influence of aggregate states promotes higher luminescence efficiency. In turn, lower yield measured for film B_4 would

be consistent with the possibility of TTA events in this most concentrated film.

When Zeonex[®] is removed (consistent with a less rigid medium) the PH of phenazine-based 1,2,3-triazole molecules in neat films is not observed. This is clearly due to a more effective vibrational quenching of the triplet population. On the other hand, delayed fluorescence (DF) was clearly observed with maximum intensity around 540 nm, *i.e.* in the aggregate form, corresponding to very long-lived singlet aggregate states, which are probably formed as a result of TTA, occurring in dimers due to better triplet mobility in neat films. It is worth mentioning that these DF spectra (Figs. 4a and 4b) are relatively noisy compared to the PH signal obtained at the same TD and IT conditions (Fig. 5a).

The detection of the DF spectra around 540 nm at $TD = 1$ ms, instead of PH spectra, is the experimental proof of the change of the dynamics of the probe neat films when compared to the blended films B_2 and B_4 . This indicates that the emission dynamics is strongly de-

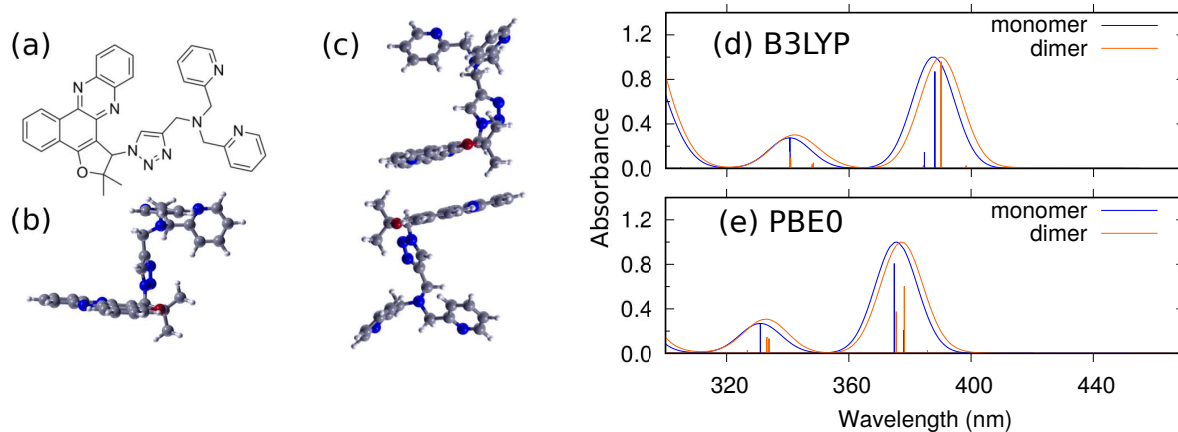


FIG. 6: (Color Online) (a) Schematic view of the monomer structure of the probe derivative phenazine molecule. In (b) and (c) are shown the optimized geometries of the monomer and dimer, respectively. In (d) and (e) are the normalized UV-Vis absorption spectra of the monomer and dimer calculated with B3LYP and PBE0 functionals, respectively.

pendent on the intermolecular interactions and/or the conformational properties of the molecular system,^{18–20} demonstrating a more detrimental effect for the emission of triplet states in neat films.

In order to investigate the structure of the aggregate form in the phenazine-based 1,2,3-triazole molecules, computational studies were performed using the density functional theory (DFT) and its time-dependent formalism (TD-DFT) as implemented as in the ORCA code version 4.0.0.²¹ The hybrid exchange correlation B3LYP functional^{22–24} with a def2-SVP²⁵ basis set was used to obtain the optimized geometries of the monomer and aggregated forms. The results clearly reveal the formation of dimer states is favoured in the phenazine-based 1,2,3-triazole molecule studied here, forming a quasi-parallel sandwich type arrangement between the two phenazines.

TD-DFT calculations were also carried out to find the electronic levels involved in the excitations and to calculate the monomer and aggregate UV-Vis spectra. Furthermore, the UV-Vis spectra were obtained with two different exchange correlation hybrid functionals: B3LYP and PBE0.²⁶ For PBE0 we used the fixed geometries obtained with B3LYP functional. In all TD-DFT calculations, the first 20 singlet excited states were calculated with a tight criteria for the convergence of the self-consistent field (SCF) iteration. To provide a simple visualization of the UV-Vis spectra, the TD-DFT excitations energies and oscillator strengths were convoluted with normalized Gaussian functions with a 8 nm full width at half maximum.

Figure 6a shows a planar schematic view of the monomer, featuring a phenazine group bonded to a N,N-bis(pyridin-2-ylmethyl)prop-2-yn-1-amine.¹⁶ The optimized geometry in **Fig. 6b** reveals its three dimensional structure, exhibiting the planar configuration of the phenazine group. The dimer was constructed by the stacking of such planar regions. Two initial con-

figurations were considered, and both converged to the same optimized geometry shown in **Fig. 6c**. The theoretical UV-Vis spectra shown in **Figs. 6d** and **6e**, despite the simple models used, are qualitatively valid for comparison purposes. For the monomer and dimer, both functionals employed led to similar UV-Vis, except for an overall violet shift in the PBE0 case relative to the B3LYP result. For the monomer, two intense electronic transitions are observed in the range of 360.0 and 400.0 nm, the most intense peak observed at 388.1 nm and at 374.9 nm in the B3LYP and PBE0 calculations, respectively. As it can be seen in *Table S1* of the supplementary material, these intense peaks may be ascribed to transitions from the HOMO-1 to LUMO, and these two orbitals are localized in the planar phenazine compound (**Fig. S2** of the supplementary material). The less intense peaks correspond to transitions from lower states to the LUMO (*Table S1* of the supplementary material). Regarding the dimer UV-Vis spectra, several electronic transitions in the range of 360.0 and 400.0 nm with vanishing oscillator strengths were identified, and the most intense electronic transitions in this range have contributions from excitations between molecular orbitals in the planar phenazine group (see *Table S2* and **Fig. S3** of the supplementary material). Furthermore, both functionals reveal a red shift in the UV-Vis spectra of the dimer in relation to the spectra of the monomer. This effect may be related to the modification of the molecular orbitals in the planar phenazine compound when the dimer is formed, lowering the energy of the orbitals and, consequently, lowering the energy of the electronic transitions. The red shift obtained with both functionals after the dimerisation is in qualitative good agreement with the experimental results. In fact, the UV-Vis spectrum for the B_4 film (**Fig. 1**), which is the most likely to form dimers, clearly suggests the existence of states shifted towards larger wavelengths (broadening effect).

IV. CONCLUSIONS

Dropcast blended films B_2 and B_4 , produced from phenazine derivative solutions of low and high concentrations respectively mixed with Zeonex[®] matrix, were investigated by time-resolved luminescence spectroscopy at room temperature. TRFL emissions around 430 nm and 540 nm, were observed at different time delays, and assigned as coming from monomer and dimer species, respectively in the film B_2 , while for the film B_4 only the dimer TRFL emission was observed. These results put in evidence the consequences of aggregation effects on the singlet emission dynamics of organic materials

No direct aggregation effects were observed on the lifetime of the triplet state, measured by the PH emission decay from films B_2 and B_4 , or the shape of their PH spectra. The PH emissions at steady state conditions, however, were observed to be more intense than the fluorescence ones, even though at room temperature.⁵ The QY of the film B_2 was also observed to be relatively higher than that of the film B_4 . The dimer formation in film B_2 it is not so predominant as it is in film B_4 . These experimental facts indicate that aggregation effects are detrimental to the emission of triplet states in organic materials.

Going further in the research of aggregation effects on the dynamics of singlet and triplet emissions we investigated neat films of derivative phenazine probe molecules. These films present higher intermolecular interaction, *i.e.*, higher aggregation effect is expected due to the absence of the Zeonex[®] matrix. However, effective electron interactions with molecular vibrational modes are enhanced, strongly favoring non-radiative emission decay. For the singlet states, increasing intermolecular interactions leads to weaker emission. This was experimentally observed for the neat films, where just singlet TRFL monomer emissions have survived at early times, independently of their low or high probe molecule concentration. For the emission taken at relatively long time delay ($TD = 1$ ms), both neat films (low and high concentra-

tions) presented a delayed and relatively weak emission due to dimer states (centered around 540 nm) instead of the expected PH emission. Considering the competing character between PH emissions with non-radiative decays due to vibrations and/or TTA, the PH is effectively quenched, as observed experimentally, due to the much higher probability of non-radiative recombination processes at room temperature in neat films.

In summary, the strong dependence of the emission dynamics of singlet and triplet states of phenazine derivatives on molecular aggregation was demonstrated in this work. The different preparation conditions of the films leads to the observation of relatively large PLQY and relatively strong room temperature phosphorescence in the more viscous films containing Zeonex[®]. In other words, films with the minimum contribution of aggregates must present enhanced photophysical properties with much lower TTA and non-radiative losses. Thus, the higher dilution of the probe molecule in Zeonex[®], as used in film B_2 , was essential to achieve these conditions. The results presented here have a direct importance concerning potential applications, in particular, purely organic phosphorescent light emitting diodes.

V. CONFLICTS OF INTEREST

There are no conflicts of interest to declare.

Acknowledgments

L. A. Cury, G. A. M. Jardim, E. N. da Silva Jr., O. J. Silveira and M. J. S. Matos thank FAPEMIG, CAPES and CNPq from Brazil for the financial support. P. L. dos Santos thanks CAPES - Science Without Borders, Brazil, for the Doctorate studentship, Proc. 12027/13-8. The authors also acknowledge Dr. Mário S. C. Mazzoni for fruitful discussions on the TD-DFT calculations.

¹ M. Más-Montoya, R. A. J. Janssen, *Adv. Funct. Mater.* 27, 1605779 (1-12) (2017).

² S. Reineke, M. A. Baldo, *Scientific Reports* 4, 3797 (2014).

³ N. Kleinhenz, N. Persson, Z. Xue, P. H. Chu, G. Wang, Z. Yuan, M. A. McBride, D. Choi, M. A. Grover, E. Reichmanis, *Chem. Mater.* 28, 3905 (2016).

⁴ S. D. Spencer, C. Bougher, P. J. Heaphy, V. M. Murcia, C. P. Gallivan, A. Monfette, J. D. Andersen, J. A. Cody, B. R. Conrad, C. J. Collison, *Solar Energy Materials & Solar Cells* 112, 202 (2013).

⁵ B. B. A. Costa, P. D. C. Souza, R. N. Gontijo, G. A. M. Jardim, R. L. Moreira, E. N. da Silva Júnior, Luiz A. Cury, *Chem. Phys. Lett.* 695, 176 (2018).

⁶ K. Hany, X. Luy, J. Xuy, G. Zhouy, S. May, W. Wangy, Z. Caiz, J. Zhouz, *J. Phys. D: Appl. Phys.* 30, 2923 (1997).

⁷ P. L. dos Santos, J. S. Ward, A. S. Batsanov, M. R. Bryce, A. P. Monkman, *The Journal of Physical Chemistry C* 121, 16462 (2017).

⁸ D. Lee, O. Bolton, B. C. Kim, J. H. Youk, S. Takayama, J. Kim, *J. Am. Chem. Soc.* 135, 6325 (2013).

⁹ S. Mukherjee, P. Thilagar, *Chem. Commun.* 51, 10988 (2015).

¹⁰ B. B. A. Costa, G. A. M. Jardim, P. L. Santos, H. D. R. Calado, A. P. Monkman, F. B. Dias, E. N. da Silva Júnior, L. A. Cury, *Phys. Chem. Chem. Phys.* 19, 3473 (2017).

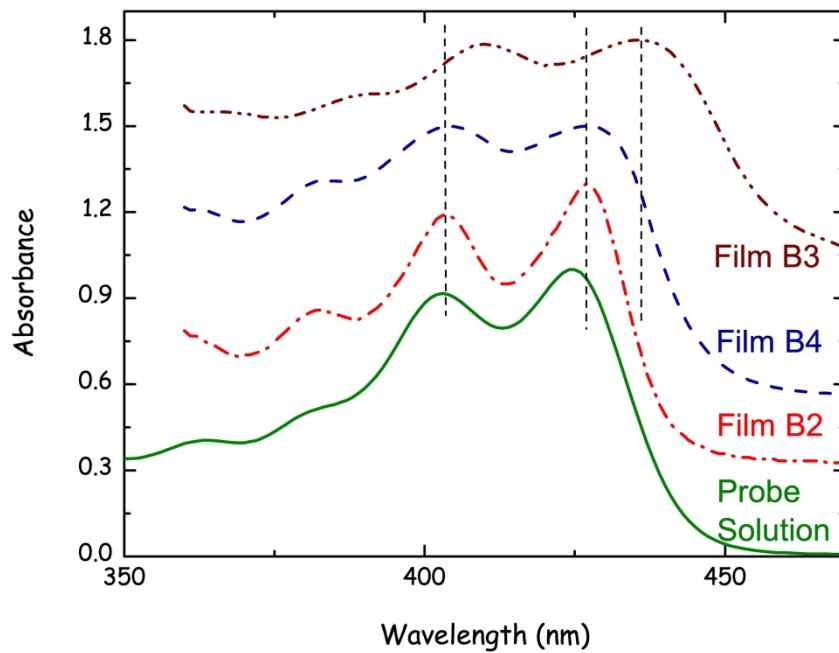
¹¹ Y. Hirata, I. Tanaka, *Chem. Phys. Lett.* 43, 568 (1976).

¹² A. Grabowska, *Chem. Phys. Lett.* 1, 113 (1967).

¹³ T. G. Pavlopoulos, *Spectrochim. Acta* 43A, 715 (1987).

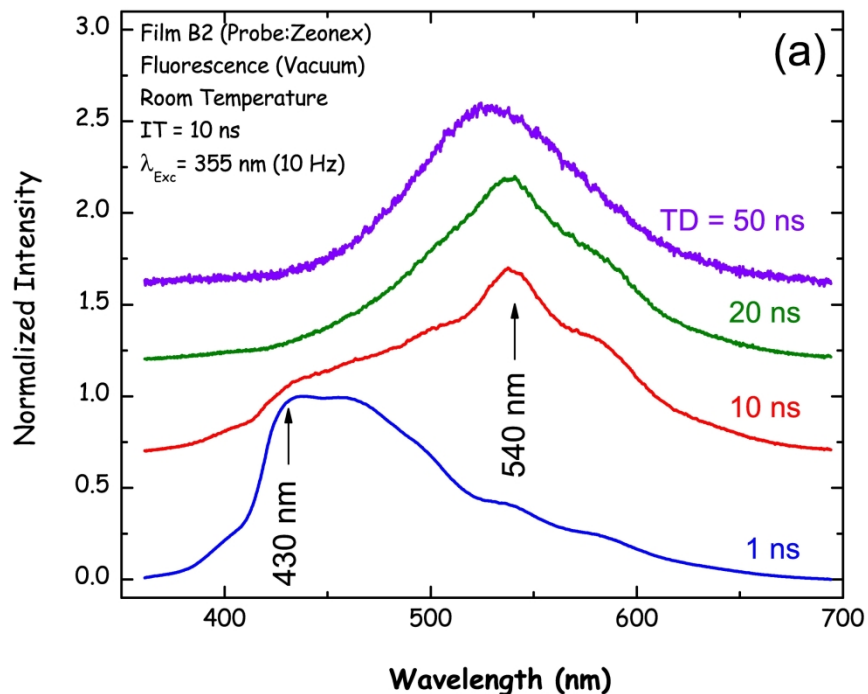
¹⁴ J. I. DelBarrio, J. R. Rebato, F. M. G. Tablas, *J. Phys. Chem.* 93, 6836 (1989).

- ¹⁵ V. A. Kuz'min, P. P. Levin, Bull. Acad. Sci. USSR Div. Chem. Sci. 37, 1098 (1988).
- ¹⁶ G. A. M. Jardim, H. D. R. Calado, L. A. Cury, E. N. da Silva Júnior, Eur. J. Org. Chem. 2015, 703 (2015) .
- ¹⁷ B. B. A. Costa, P. L. Santos, M. D. R. Silva, S. L. Nogueira, K. A. S. Araujo, B. R. A. Neves, T. Jarrosson, F. Serein-Spirau, J.-P. Lére-Porte, L. A. Cury, Chem. Phys. Lett. 614, 67 (2014).
- ¹⁸ H. H. Billsten, V. Sundström, T. Polívka, J. Phys. Chem. A 109, 1521 (2005).
- ¹⁹ H. H. Billsten, D. Zigmantas, V. Sundström, T. Polívka, Chem. Phys. Lett. 355, 465 (2002).
- ²⁰ M. Durchan, M. Fuciman, V. Šlouf, G. Kesan, T. Polivka, J. Phys. Chem. A 116, 12330 (2012).
- ²¹ F. Neese, WIREs Comput. Mol. Sci. 2, 73 (2012).
- ²² A. D. Becke, Phys. Rev. A 38, 3098 (1988).
- ²³ C. Lee, W. Yang, R. G. Parr, Phys. Rev. B 37, 785 (1988).
- ²⁴ A. D. Becke, J. Chem. Phys. 98, 5648 (1993).
- ²⁵ A. Schafer, H. Horn, R. Ahlrichs, J. Chem. Phys. 97, 2571 (1992).
- ²⁶ C. Adamo, V. Barone, J. Chem. Phys. 110, 6158 (1999).



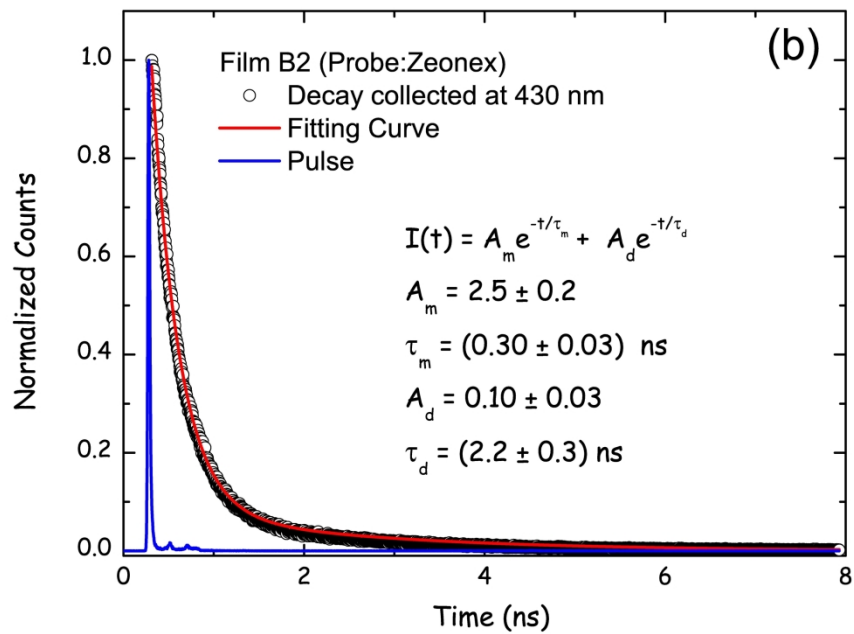
The normalized UV-Vis absorption spectra for the neat film B3 (dashed-dotted-dotted line), for the probe:ZeonexR blended film B4 (dashed line), for the probe:ZeonexR blended film B2 (dashed-dotted line), and for the solution of the probe molecule at 0.1 mg/mL in CHCl_3 (solid line), at room temperature. The spectra were displaced from each other for clarity sake.

267x214mm (300 x 300 DPI)

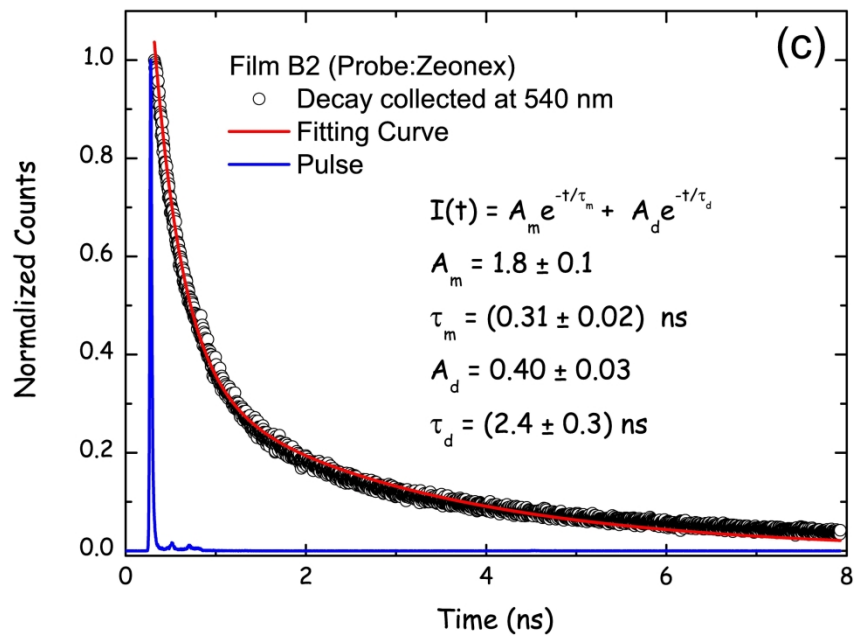


(a) Time resolved fluorescence (TRFL) spectra obtained for the film B2 at time delays (TDs) of 1 ns, 10 ns, 20 ns and 50 ns. The TRFL measurements were performed at room temperature, under vacuum, with the excitation made by a 355 nm pulsed laser line (repetition rate of 10 Hz). The spectra were normalized and displaced from each other for clarity sake. The integration time (IT) of 10 ns was used in all measurements; (b) Time correlated single photon counting (TCSPC) decay obtained for the film B2 with emission collected at 430 nm; (c) TCSPC decay obtained for the film B2 with emission collected at 540 nm. The TCSPC decays were obtained with the excitation made by a second harmonic pulsed laser ($\lambda = 394$ nm, 76 MHz of repetition rate) from a mode-locked Ti:sapphire laser, Coherent Inc.. The corresponding lifetime components (τ_1 and τ_2), obtained by fitting the decay data (solid lines) in (b) and (c), are shown in the respective insets. Deconvolution process of the decays in parts (b) and (c) were not considered due to the relatively low instrument response function (IRF) of the TCSPC system (24 ps). The pulse curves in (b) and (c), representing the IRF, are shown just for the completeness sake.

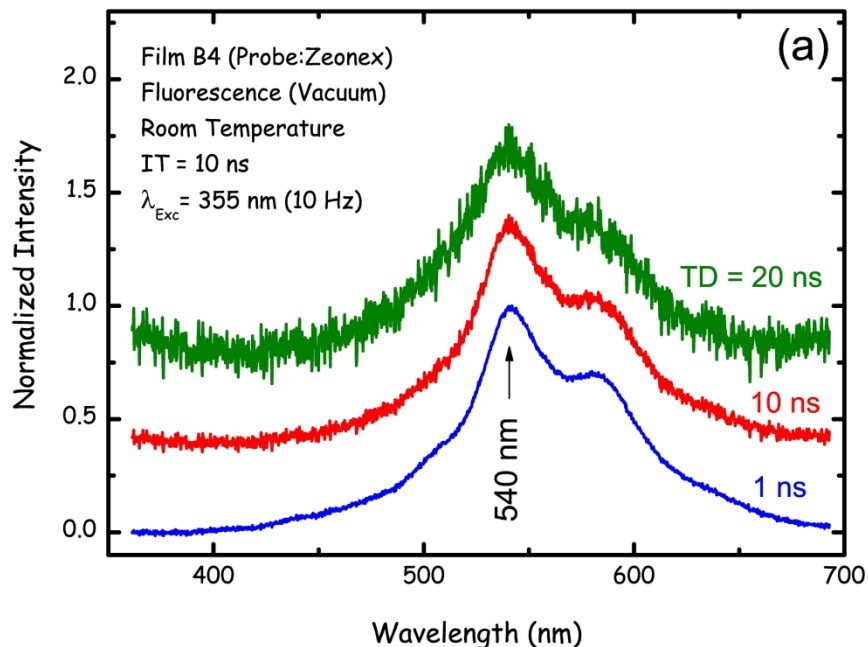
263x224mm (300 x 300 DPI)



267x212mm (300 x 300 DPI)



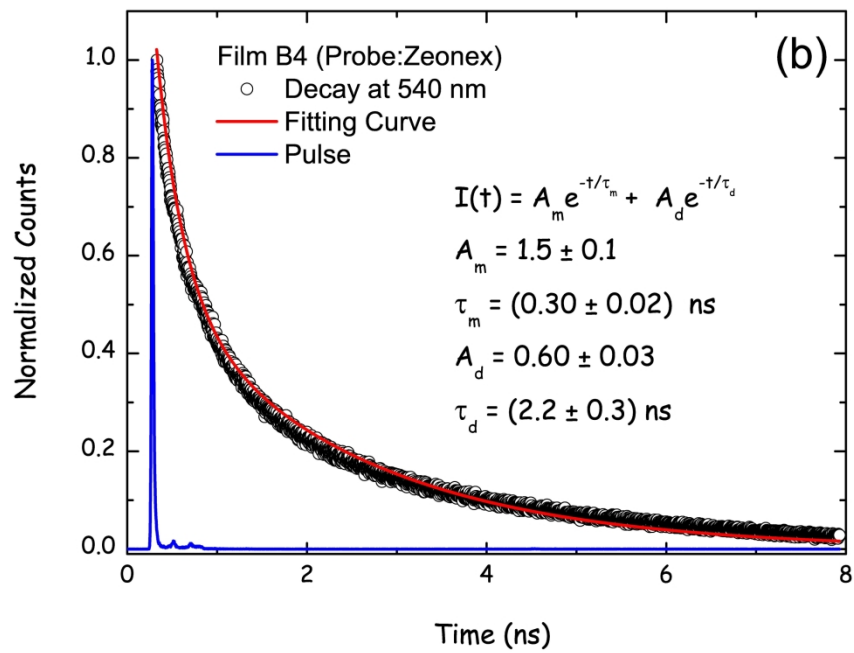
267x212mm (300 x 300 DPI)



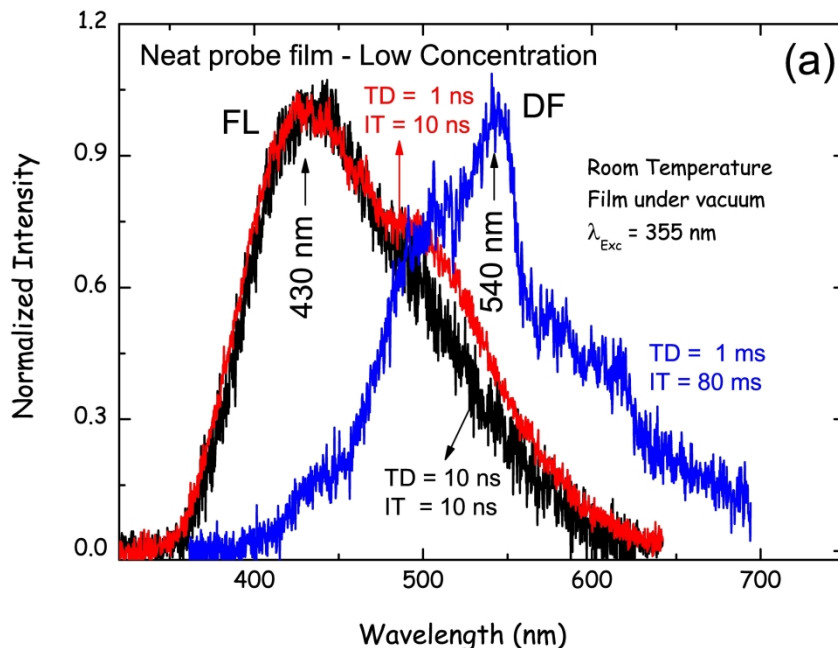
(a) TRFL spectra obtained for the film B4 at time delays (TD) of 1 ns, 10 ns, and 20 ns. The TRFL measurements were performed at room temperature, under vacuum, with the excitation made by a 355 nm pulsed laser line (repetition rate of 10 Hz). The spectra were normalized and displaced from each other for clarity sake. The integration time (IT) of 10 ns was used in all measurements; (b) Time correlated single photon counting (TCSPC) decay obtained for the film B4 at 540 nm. The TCSPC decay was obtained with the excitation made by a second harmonic pulsed laser ($\lambda = 394 \text{ nm}$, 76 MHz of repetition rate) from a mode-locked Ti:sapphire laser, Coherent Inc.. The corresponding lifetime components (m and d), obtained by fitting the decay data (solid line), are shown in the inset. Deconvolution process of the decay in part (b) was not considered due to the relatively low instrument response function (IRF) of the TCSPC system (24 ps).

The pulse curve in (b), representing the IRF, is shown just for the completeness sake.

269x216mm (300 x 300 DPI)

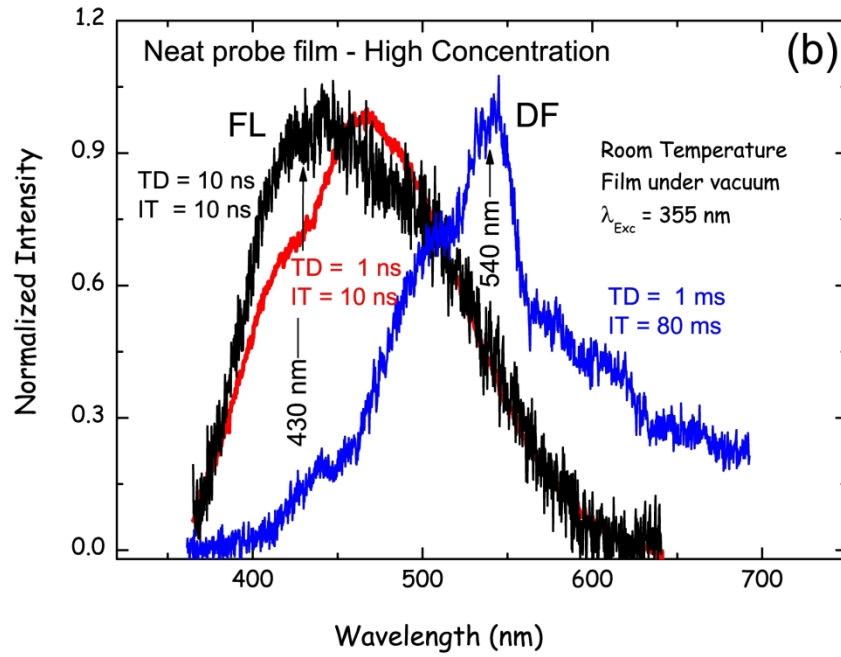


268x215mm (300 x 300 DPI)

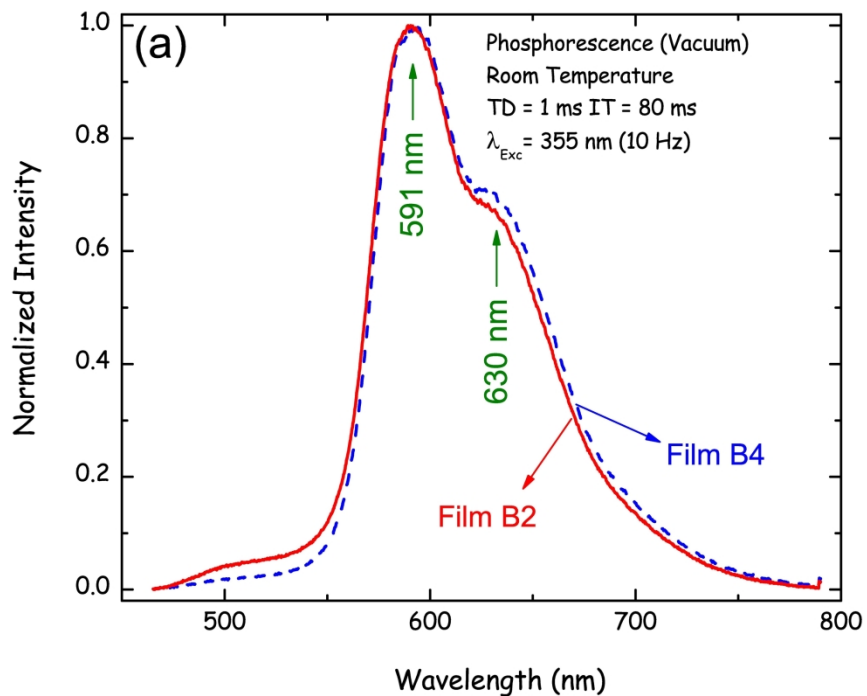


(a) Normalized time resolved fluorescence (TRFL) spectra of the probe neat film made from the low concentration (0.1 mg/mL) probe solution at TD = 1 ns and 10 ns with IT = 10 ns, and the delayed fluorescence (DF) spectrum at TD = 1 ms and IT = 80 ms; (b) Normalized TRFL spectra of the probe neat film made from the high concentration (3.4 mg/mL) probe solution at TD = 1 ns and 10 ns with IT = 10 ns, and the DF spectrum at TD = 1 ms and IT = 80 ms. The measurements of TRFL and DF spectra in (a) and in (b) were performed at room temperature, under vacuum, with the excitation made by a 355 nm pulsed laser line (repetition rate of 10 Hz).

273x215mm (300 x 300 DPI)

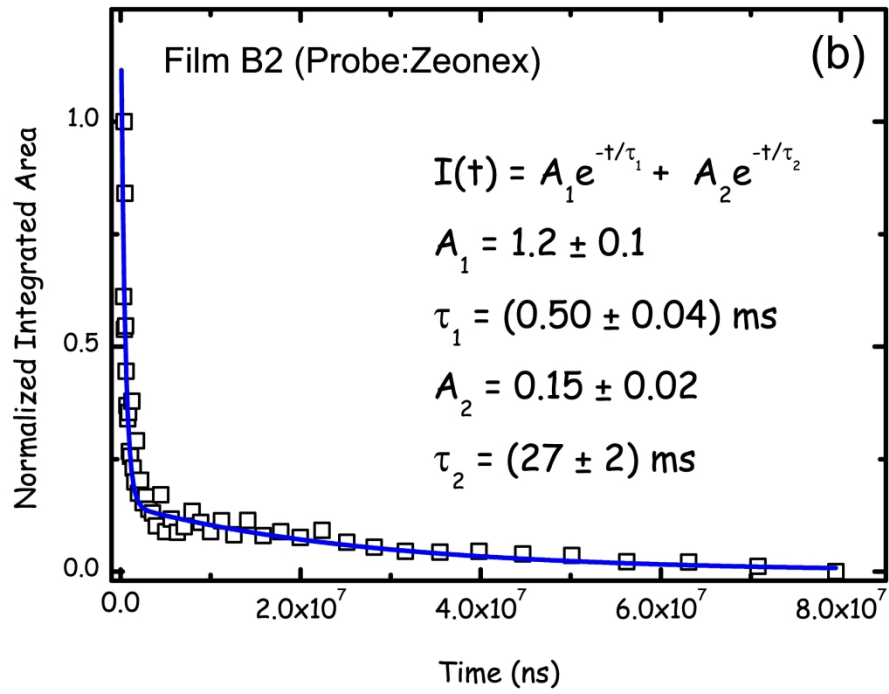


271x216mm (300 x 300 DPI)

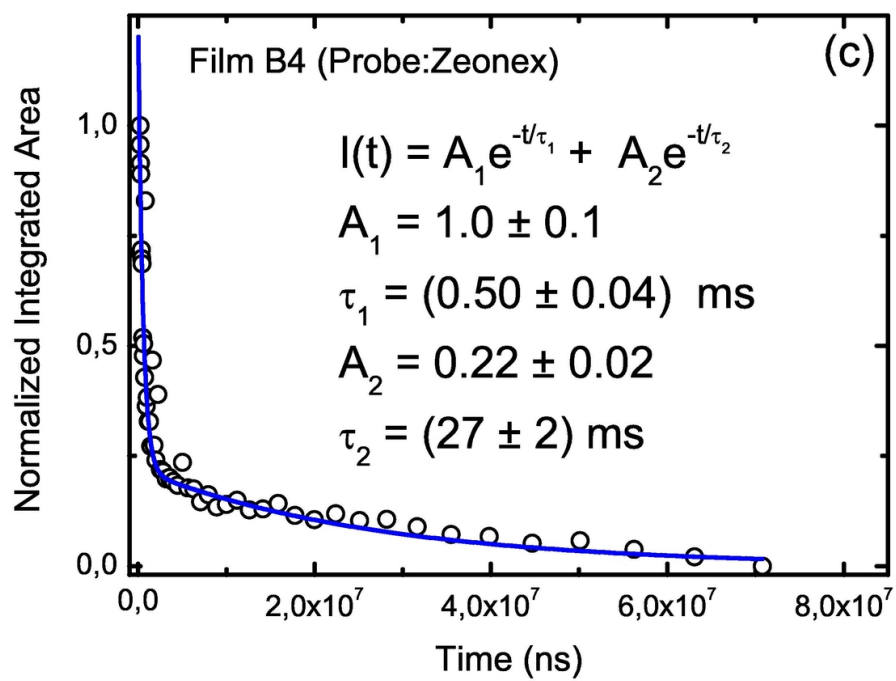


(a) Normalized Phosphorescence (PH) spectra obtained from gated fluorescence for the B2 and B4 films using TD = 1 ms and IT = 80 ms; (b) and (c) are respectively the PH Decay curves of the B2 (squares) and B4 (circles) films obtained by gated fluorescence. The corresponding lifetime components ($i, i = 1, 2$), obtained from the fitting of the respective decay data (dashed lines), are shown in the respective inset. The measurements of PH spectra in (a) and the PH decays in (b) and (c) were performed at room temperature, under vacuum, with the excitation made by a 355 nm pulsed laser line (repetition rate of 10 Hz).

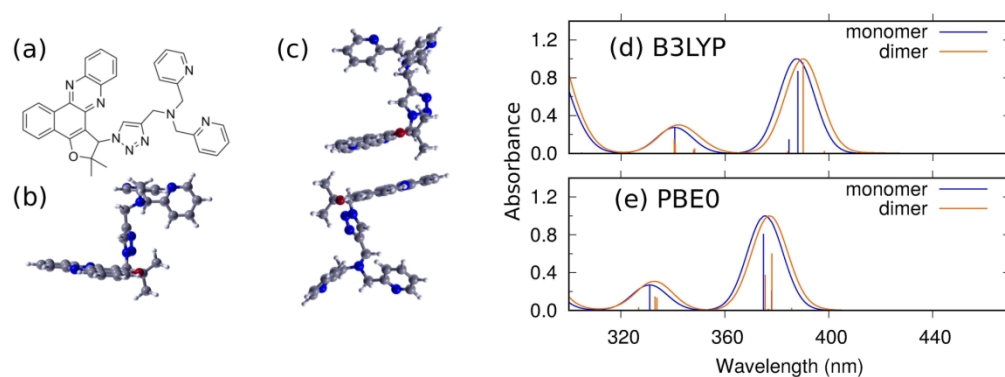
264x223mm (300 x 300 DPI)



256x204mm (300 x 300 DPI)



104x81mm (300 x 300 DPI)



(a) Schematic view of the monomer structure of the probe derivative phenazine molecule. In (b) and (c) are shown the optimized geometries of the monomer and dimer, respectively. In (d) and (e) are the normalized UV-Vis absorption spectra of the monomer and dimer calculated with B3LYP and PBE0 functionals, respectively.

175x68mm (300 x 300 DPI)

Dynamics of aggregated states resolved by gated fluorescence in films of room temperature phosphorescent emitters

Paloma L. dos Santos¹, Orlando J. Silveira², Rongjuan Huang¹, Guilherme A. M. Jardim³, Matheus J. S. Matos⁴, Eufrânio N. da Silva Júnior³, Andrew P. Monkman¹, Fernando B. Dias¹, Luiz A. Cury²

¹Department of Physics, University of Durham, South Road DH1 3LE, Durham, United Kingdom

²Instituto de Ciências Exatas, Departamento de Física, Universidade Federal de Minas Gerais, 31270-901, Belo Horizonte, Minas Gerais, Brazil

³Instituto de Ciências Exatas, Departamento de Química, Universidade Federal de Minas Gerais, 31270-901, Belo Horizonte, Minas Gerais, Brazil

⁴Instituto de Ciências Exatas e Biológicas, Departamento de Física, Universidade Federal de Ouro Preto, 35400-000, Ouro Preto, Minas Gerais, Brazil

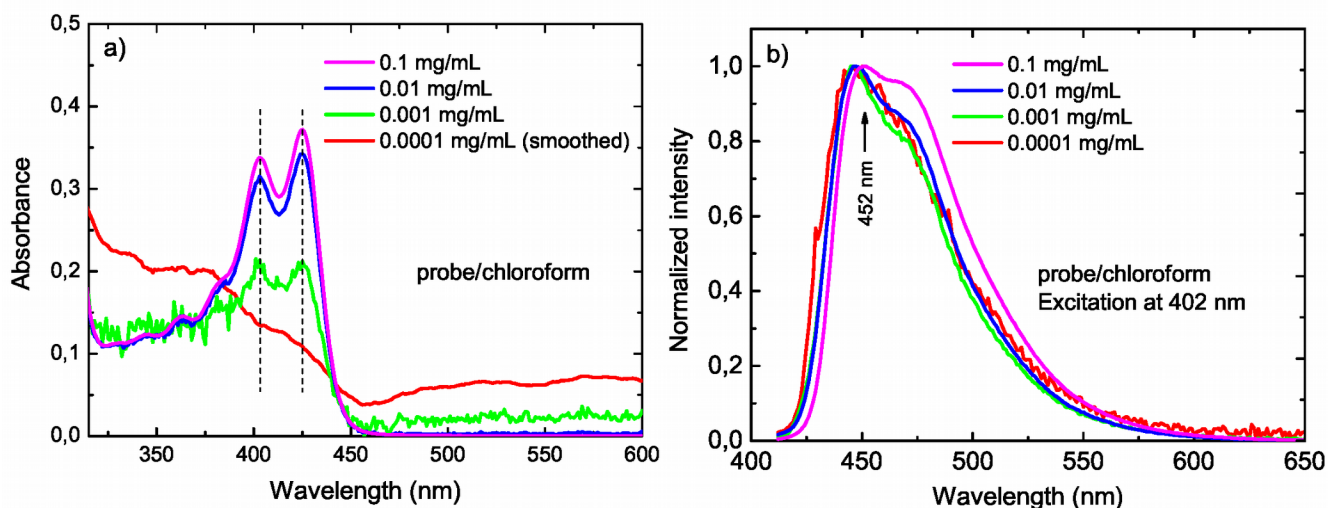


Figure S1: (a) Absorption and (b) Emission spectra at relatively low concentration of probe solutions in chloroform.

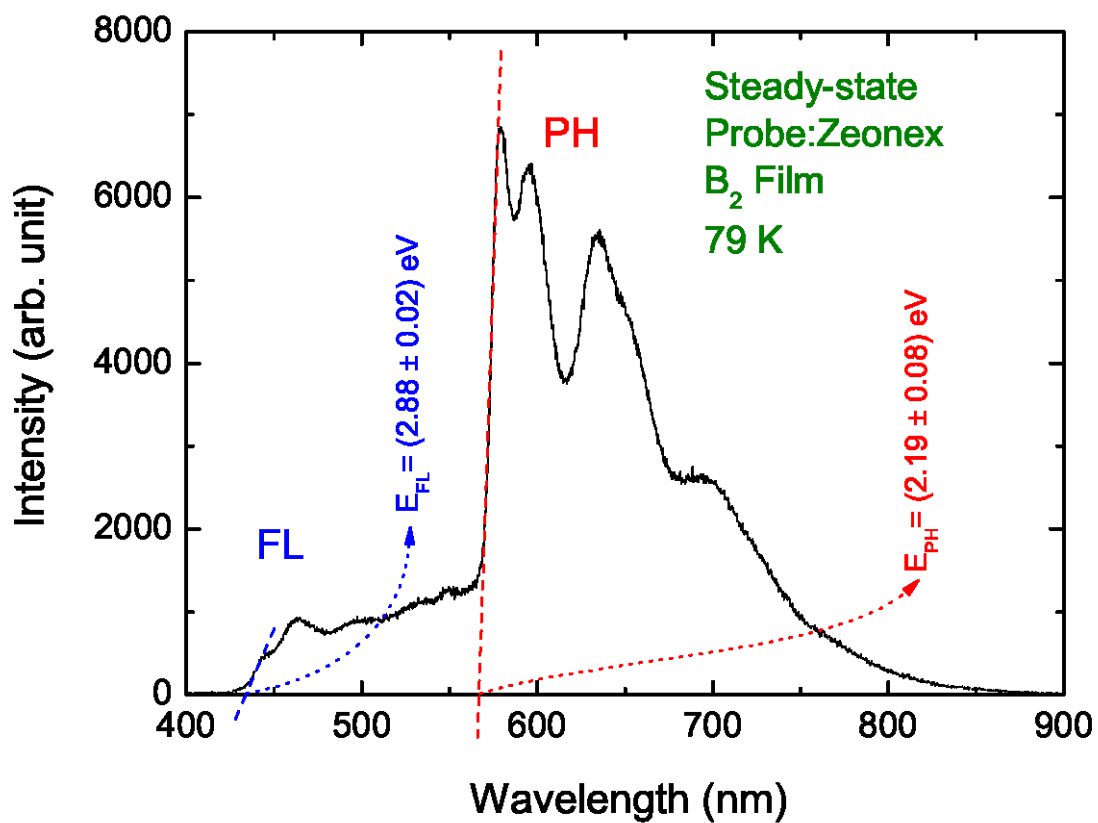


Figure S2: Steady-state emission spectrum of film B2 at 79 K. The FL and PH energies, indicated by arrows, were estimated from the respective onset lines.

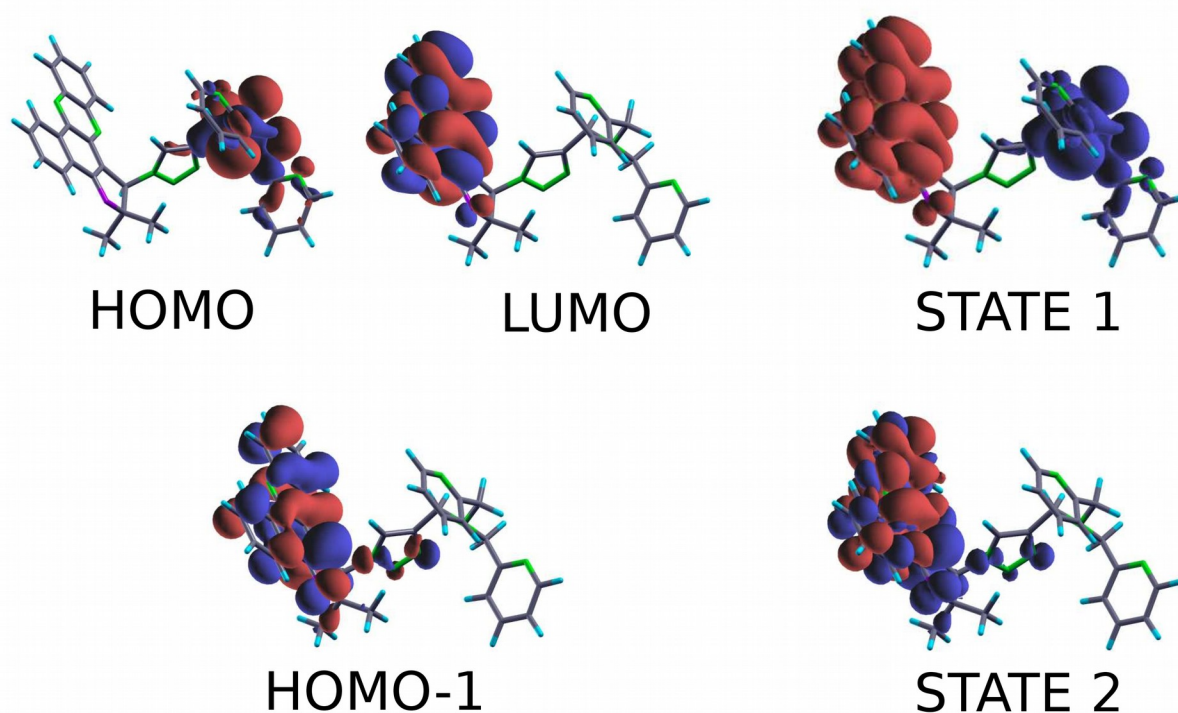


Figure S3: Molecular orbital plots for the HOMO-1, HOMO and LUMO of the monomer and the TDDFT difference densities for state 1 and 2 calculated with the B3LYP functional. In TDDFT difference densities, blue indicates a loss of electron density upon excitation and red indicates a gain of electron density. The TDDFT difference density for state 1 indicates an excitation from a molecular orbital localized on the N,N-bis(pyridin-2-ylmethyl)prop-2-yn-1-amine (HOMO) to a molecular orbital on the planar phenazine compound (LUMO), and exhibits very small oscillator strength (Table 1). The state 2 shows the TDDFT difference density for the transition from HOMO-1 to LUMO, which corresponds to an excitation localized on the phenazine compound plane and contribute to an intense peak on the UVvis spectrum. The molecular orbitals obtained with PBE0 are very similar, so the TDDFT difference densities must not differ.

Table S1: Energy λ (in nm), oscillator strength f_{osc} , and orbitals that have relevant contributions to the electronic transitions of the monomer calculated with TDDFT/B3LYP and TDDFT/PBE0 (PBE0 calculation with fixed geometry from B3LYP). In main transitions, the orbitals 151 and 152 are the HOMO and LUMO, respectively.

state	B3LYP			PBE0		
	λ (nm)	f_{osc}	Main transitions ($\geq 10\%$)	λ (nm)	f_{osc}	Main transitions ($\geq 10\%$)
1	455.6	0.0000	151 \rightarrow 152 (100%)	420.4	0.0000	151 \rightarrow 152 (100%)
2	388.1	0.1244	147 \rightarrow 152 (12%) 150 \rightarrow 152 (74%)	378.1	0.0353	145 \rightarrow 152 (25%) 147 \rightarrow 152 (43%) 150 \rightarrow 152 (18%)
3	384.9	0.0259	147 \rightarrow 152 (65%) 150 \rightarrow 152 (14%)	374.9	0.1351	147 \rightarrow 152 (11%) 150 \rightarrow 152 (70%)
4	340.6	0.0406	149 \rightarrow 152 (71%) 150 \rightarrow 153 (22%)	331.0	0.0450	149 \rightarrow 152 (72%) 150 \rightarrow 153 (21%)

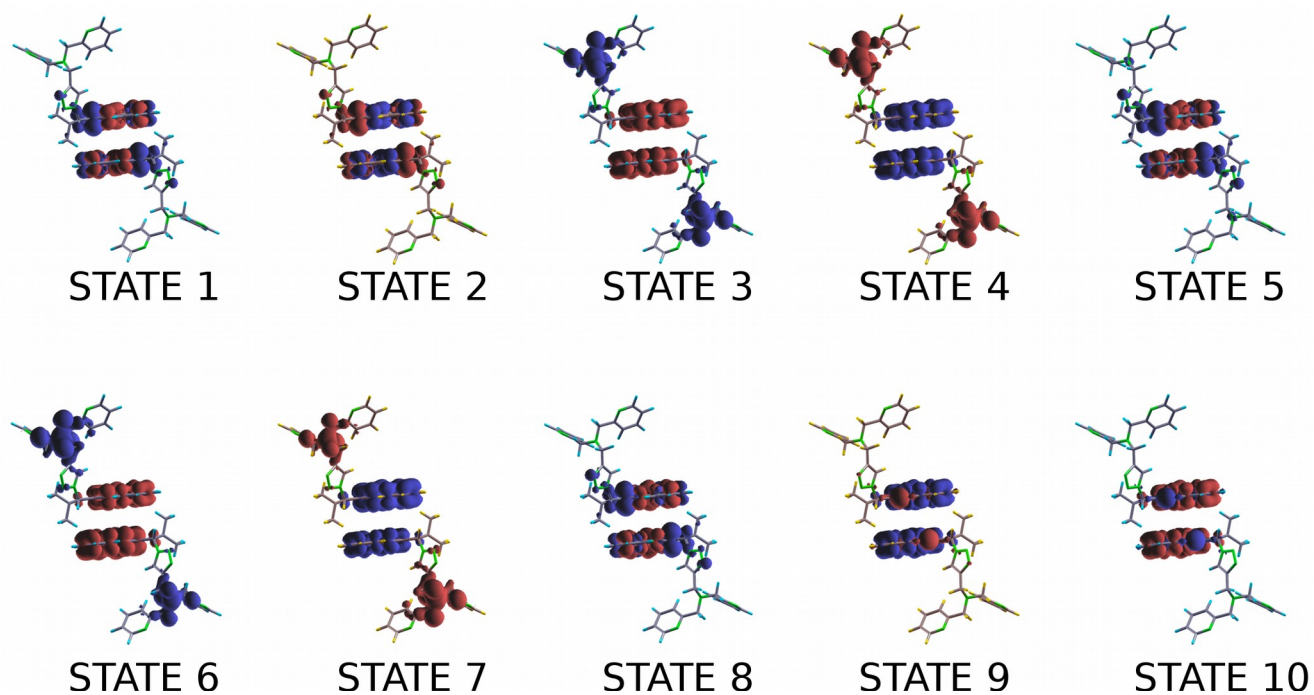


Figure S4: TDDFT difference densities for state 1 to 10 of the dimer calculated with the B3LYP functional. In TDDFT difference densities, blue indicates a loss of electron density upon excitation and red indicates a gain of electron density. The molecular orbitals obtained with PBE0 are very similar, so the TDDFT difference densities must not differ.

Table S2: Energy λ (in nm), oscillator strength f_{osc} , and orbitals that have relevant contributions to the electronic transitions of the dimer calculated with TDDFT/B3LYP and TDDFT/PBE0 (PBE0 calculation with fixed geometry from B3LYP). For the dimer, several molecular orbitals are degenerated, for example, 302 and 303 orbitals are the HOMO while the 304 and 305 are the LUMO. The 300 and 301 orbitals have contribution on several main transitions shown in this Table, and both are the degenerate HOMO-1.

state	B3LYP			PBE0		
	λ (nm)	f_{osc}	Main transitions ($\geq 10\%$)	λ (nm)	f_{osc}	Main transitions ($\geq 10\%$)
1	417.5	0.0000	300 \rightarrow 304 (53%) 301 \rightarrow 305 (45%)	393.2	0.0009	300 \rightarrow 304 (54%) 301 \rightarrow 305 (42%)
2	417.4	0.0005	300 \rightarrow 305 (44%) 301 \rightarrow 304 (54%)	393.2	0.0008	300 \rightarrow 305 (36%) 301 \rightarrow 304 (60%)
3	406.2	0.0003	302 \rightarrow 304 (10%) 303 \rightarrow 305 (11%) 302 \rightarrow 305 (36%) 303 \rightarrow 304 (43%)	385.7	0.0061	300 \rightarrow 305 (55%) 301 \rightarrow 304 (31%)
4	406.1	0.0008	302 \rightarrow 304 (43%) 303 \rightarrow 305 (36%) 302 \rightarrow 305 (11%) 303 \rightarrow 304 (10%)	378.1	0.1335	300 \rightarrow 304 (19%) 301 \rightarrow 305 (23%) 302 \rightarrow 304 (14%) 303 \rightarrow 305 (14%)
5	398.3	0.0314	300 \rightarrow 305 (50%) 301 \rightarrow 304 (40%)	377.0	0.0027	288 \rightarrow 305 (21%) 289 \rightarrow 304 (19%) 302 \rightarrow 305 (20%) 303 \rightarrow 304 (23%)
6	392.7	0.0000	302 \rightarrow 304 (30%) 303 \rightarrow 304 (16%) 303 \rightarrow 305 (47%)	377.0	0.0006	288 \rightarrow 304 (17%) 289 \rightarrow 305 (14%) 302 \rightarrow 304 (28%) 303 \rightarrow 305 (26%)
7	392.7	0.0000	302 \rightarrow 304 (16%) 302 \rightarrow 305 (47%) 303 \rightarrow 304 (30%)	376.6	0.0029	288 \rightarrow 305 (17%) 389 \rightarrow 304 (15%) 302 \rightarrow 305 (24%) 303 \rightarrow 304 (26%)
8	390.1	0.2251	300 \rightarrow 304 (39%) 301 \rightarrow 305 (46%)	375.5	0.0832	288 \rightarrow 304 (14%) 289 \rightarrow 305 (11%) 300 \rightarrow 304 (18%) 301 \rightarrow 305 (25%)
9	384.3	0.0072	290 \rightarrow 305 (35%) 291 \rightarrow 304 (33%) 293 \rightarrow 304 (14%)	362.6	0.0000	302 \rightarrow 304 (24%) 302 \rightarrow 305 (15%) 303 \rightarrow 304 (22%) 303 \rightarrow 305 (36%)
10	384.0	0.0045	290 \rightarrow 304 (36%) 291 \rightarrow 305 (31%) 293 \rightarrow 305 (13%)	362.6	0.0000	302 \rightarrow 304 (22%) 302 \rightarrow 305 (36%) 303 \rightarrow 304 (24%) 303 \rightarrow 305 (15%)